REPORT DOCUM

AD-A223 853

Form Approved
OMB No. 0704-0188

1. AGENCY USE ONLY (Leave blank)	2. REPORT DATE	3. REPORT TYPE AND DATES COVERED
	June 1990	Paper, Oct 85 - Apr 90

4. TITLE AND SUBTITLE

Cavity Aeroacoustics

5. FUNDING NUMBERS

PE 62602F

PR 2567
TA 03
WU 20

6. AUTHOR(S)

Richard E. Dix, Carroll Butler

7. PERFORMING ORGANIZATION NAME(S) AND ADDRESS(ES)

Calspan Corporation, AEDC Operations
Arnold Air Force Base, TN

8. PERFORMING ORGANIZATION REPORT NUMBER

DTIC ELECTE JUL 0 6 1990 S D

9. SPONSORING/MONITORING AGENCY NAME(S) AND ADDRESS(ES)

Aerodynamics Branch
Aeromechanics Division (AFATL/FXA)
Air Force Armament Laboratory
Eglin AFB, FL 32542-5434.

10. SPONSORING/MONITORING AGENCY REPORT NUMBER

AFATL-TP-90-08

11. SUPPLEMENTARY NOTES

Technical paper presented at Store Carriage, Interaction and Release Conference, Bath, England

12a. DISTRIBUTION/AVAILABILITY STATEMENT

Approved for public release; distribution is unlimited.

12b. DISTRIBUTION CODE

13. ABSTRACT (Maximum 200 words)

Two important flow phenomena occur with exposure of a cavity in high speed aircraft: 1)development of a shear layer within which transition from the stagnant cavity environment to the active external flow occurs, and 2)the creation of a concomitant fluctuating pressure environment. A program of experiments has been undertaken since 1985 at Arnold AFB, TN, to investigate these phenomena which have resulted in a rather large data base describing the aeroacoustic environment associated with cavities of three different length-to-height (L/H) ratios, equipped with a variety of acoustic suppression devices and doors, and exposed to external flows of subsonic and supersonic speeds. This paper documents that series of experiments and the results therein.

Keywords:

14. SUBJECT TERMS

Cavity, aeroacoustics, flow suppression devices; shear layer; aeroacoustic modulation; store loads; computational fluid dynamics, Schlieren evidence.

15. NUMBER OF PAGES

34

16. PRICE CODE

17. SECURITY CLASSIFICATION OF REPORT	18. SECURITY CLASSIFICATION OF THIS PAGE	19. SECURITY CLASSIFICATION OF ABSTRACT	20. LIMITATION OF ABSTRACT
Unclassified	Unclassified	Unclassified	SAR

NSN 7540-01-280-5500

Standard Form 298 (Rev 2-89)
Prescribed by ANSI Std Z39-18
298-102

DTIC FILE COPY

90 07 1 5 087

GENERAL INSTRUCTIONS FOR COMPLETING SF 298

The Report Documentation Page (RDP) is used in announcing and cataloging reports. It is important that this information be consistent with the rest of the report, particularly the cover and title page. Instructions for filling in each block of the form follow. It is important to ***stay within the lines*** to meet ***optical scanning requirements***.

Block 1. Agency Use Only *(Leave blank)*.

Block 2. Report Date. Full publication date including day, month, and year, if available (e.g. 1 Jan 88). Must cite at least the year.

Block 3. Type of Report and Dates Covered. State whether report is interim, final, etc. If applicable, enter inclusive report dates (e.g. 10 Jun 87 - 30 Jun 88).

Block 4. Title and Subtitle. A title is taken from the part of the report that provides the most meaningful and complete information. When a report is prepared in more than one volume, repeat the primary title, add volume number, and include subtitle for the specific volume. On classified documents enter the title classification in parentheses.

Block 5. Funding Numbers. To include contract and grant numbers; may include program element number(s), project number(s), task number(s), and work unit number(s). Use the following labels:

C	- Contract	PR	- Project
G	- Grant	TA	- Task
PE	- Program Element	WU	- Work Unit Accession No.

Block 6. Author(s). Name(s) of person(s) responsible for writing the report, performing the research, or credited with the content of the report. If editor or compiler, this should follow the name(s).

Block 7. Performing Organization Name(s) and Address(es). Self-explanatory.

Block 8. Performing Organization Report Number. Enter the unique alphanumeric report number(s) assigned by the organization performing the report.

Block 9. Sponsoring/Monitoring Agency Name(s) and Address(es). Self-explanatory.

Block 10. Sponsoring/Monitoring Agency Report Number. *(If known)*

Block 11. Supplementary Notes. Enter information not included elsewhere such as: Prepared in cooperation with...; Trans. of...; To be published in... When a report is revised, include a statement whether the new report supersedes or supplements the older report.

Block 12a. Distribution/Availability Statement. Denotes public availability or limitations. Cite any availability to the public. Enter additional limitations or special markings in all capitals (e.g. NOFORN, REL, ITAR).

- **DOD** - See DoDD 5230.24, "Distribution Statements on Technical Documents."
- **DOE** - See authorities.
- **NASA** - See Handbook NHB 2200.2.
- **NTIS** - Leave blank.

Block 12b. Distribution Code.

- **DOD** - Leave blank.
- **DOE** - Enter DOE distribution categories from the Standard Distribution for Unclassified Scientific and Technical Reports.
- **NASA** - Leave blank.
- **NTIS** - Leave blank.

Block 13. Abstract. Include a brief *(Maximum 200 words)* factual summary of the most significant information contained in the report.

Block 14. Subject Terms. Keywords or phrases identifying major subjects in the report.

Block 15. Number of Pages. Enter the total number of pages.

Block 16. Price Code. Enter appropriate price code *(NTIS only)*.

Blocks 17. - 19. Security Classifications. Self-explanatory. Enter U.S. Security Classification in accordance with U.S. Security Regulations (i.e., UNCLASSIFIED). If form contains classified information, stamp classification on the top and bottom of the page.

Block 20. Limitation of Abstract. This block must be completed to assign a limitation to the abstract. Enter either UL (unlimited) or SAR (same as report). An entry in this block is necessary if the abstract is to be limited. If blank, the abstract is assumed to be unlimited.

CAVITY AEROACOUSTICS*

Richard E. Dix
Calspan Corporation, AEDC Operations
Arnold Air Force Base, Tennessee
and
Carroll Butler
AFATL/FXA, Eglin AFB, Florida

INTRODUCTION

Aircraft design decisions often depend on the two factors, weight and drag. Since the first powered flight, aircraft designers have smoothed, faired, retracted, and hidden as many external excrescences as possible in the quest for additional vehicle performance and efficiency. However, the jocular observation that "there is no free lunch" becomes a real conclusion as the designer dutifully pursues the aerodynamic grail. As an example, consider the retraction or hiding of items in a cavity that is closed and smooth to the flow over the body. At an appropriate time, doors or panels open as part of a desired operational sequence, and the storage volume, or cavity, together with the contents, are exposed to the external flow. Regardless of the purpose or contents of the cavity, two of the important flow phenomena that occur with exposure of the cavity are: 1) the development of a shear layer within which the transition occurs from the stagnant cavity environment to the active external flow; and 2) the creation of a concomitant fluctuating pressure environment in the cavity. The fluctuations often resonate at characteristic frequencies, and are generally detectable as audible tones, leading to the term "aeroacoustic" to describe the fluid dynamic environment. Over the years, various investigators have focused on the action of the shear layer passing over the cavity (a vortex-acoustic coupling) as a cause of the aeroacoustic phenomena (Refs. 1-3). In 1970, Covert (Ref. 4) offered a good historical perspective, citing Strouhal, Rayleigh, and Kohlrausch in works dating back to the 1870s, 1880s, and 1890s. More recently, Stallings and Wilcox (Ref. 5) at NASA/Langley summarized current models of supersonic flow over shallow (closed flow), medium (transitional flow), and deep (open flow) cavities, illustrated in Fig. 1.

Many sets of experiments have been completed in studies of the cavity aeroacoustic environment, among these Rossiter's predictions of the modal frequencies (Ref. 6) and Clark's studies of techniques of controlling the modal amplitudes (Ref. 7). The effect of cavity shape on the static pressure distribution over the surfaces of the cavity was reported by Plentovich (Ref. 8), and Stallings and Wilcox (Ref. 5), and computational fluid dynamic (CFD) efforts to predict cavity flow fields have been described by Suhs (Ref. 9), Rizzetta (Ref. 10), and Baysal (Ref. 11). These documents represent only a fraction of the active authors and programs setting about to better define, predict, and interact with cavity aeroacoustic phenomena. The present paper, for example, documents a program of experiments that has been underway for three years at the Arnold Engineering Development Center (AEDC), and has resulted in a rather large data base describing the aeroacoustic environment associated with cavities of three different length-to-height ratios (L/H), equipped with a variety of acoustic suppression devices and doors, and exposed to external flows of subsonic to supersonic speeds.

* The research reported herein was performed by the Arnold Engineering Development Center (AEDC), Air Force Systems Command. Work and analysis for this research were done by personnel of Calspan Corporation/AEDC Operations, operating contract for the AEDC aerospace flight dynamics facilities. Further reproduction is authorized to satisfy needs of the U. S. Government.

SHEAR LAYER

Aerodynamic Loads

Both the presence of the shear layer between the open cavity volume and the external flow field and the existence of tones in the cavity represent challenges to aircraft and systems designers. If, for instance, it is desired to move a body out of a cavity, the variation of aerodynamic forces acting on the body as it passes through the shear layer must be known. In 1983, Stallings at NASA/Langley reported large changes in loads acting on a store passing through a cavity shear layer (Ref. 12). The loads were noted to depend on the length-to-height ratio (L/H) of the cavity, Fig. 2. Using a device designed to translate the body in small increments along one axis only (the "Z-Rig," Ref. 13, Fig. 3), Dix at the Arnold Engineering Development Center (AEDC) confirmed the existence of substantial gradients in body loads when passing through the shear layer, Fig. 4 (Ref. 13). The importance of the gradients must be assessed case by case, but one must clearly proceed with caution if tempted to construct a simple curve through three data points measured at coarse intervals as indicated in Fig. 4.

Strong variations in aerodynamic loads could affect somewhat the structural integrity of any body passing through a shear layer, but perhaps the most critical question is the influence on the trajectory of a body released inside the cavity and passing outward through the shear layer. At the AEDC, Dix has measured and calculated trajectories of a store jettisoned out of a cavity. Trajectories were measured using the Captive Trajectory Support (CTS) system in the 4-ft transonic wind tunnel AEDC Aerodynamic Wind Tunnel (4T), Fig. 5 and Ref. 14. Several sets of cavity dimensions (L/H), cavity door configurations, and flow suppression devices were used to vary the configuration of the cavity, but the ejection conditions were constant. Store motion was predicted from a point at the end of a Z-axis ejector stroke. The end-of-stroke translational velocity (V_{Zeos}) was 30 ft/sec in the Z-axis direction (down and away from the cavity), and the angular pitching velocity of the store was -1 rad/sec (nose down). During the same test, aerodynamic loads acting on the store at a spatial grid of locations in and near the cavity were recorded to provide a basis for predictions of store separation trajectories using post-test computational techniques. The post-test computer code, developed by Morgret (Ref. 15) called the Multiple Degree-of-freedom Interpolation and Trajectory Generation Program, or MDITGP, is in fact a code similar to the code used to predict trajectories in the wind tunnel using the CTS system. During a test, forces and moments acting on the store in the wind tunnel are used as inputs to the code, while for the post-test trajectory predictions, the store loads inputs are interpolated from the grid data. A clear advantage of the post-test computational technique is the ease with which initial conditions, such as the end-of-stroke store velocities, can be changed to predict many different trajectories from the same set of wind tunnel data. A description of the MDITGP is contained in Ref. 15.

Using different end-of-stroke store velocities, it was possible to gain an appreciation of the effect of a cavity shear layer on the trajectory of a jettisoned store. As illustrated in Fig. 6, with the end-of-stroke Z-axis translational velocity above approximately 1.5 percent of the free-stream velocity, store motion was negligibly affected by passing through the shear layer, so long as the end-of-stroke pitch velocity, θ, was -1 rad/sec (nose-down). When the initial pitch rate of the store was $-1 < \theta \leq 0$ (or even worse, nose-up, $\theta > 0$), passage through the shear layer was not smooth, and jettison under these conditions would not be considered safe. Clearly, to assure reliable traverse through the shear layer at all jettison conditions, the store would have to be constrained in some way, such as with the use of a trapeze, a device dating back at least as far as the JU 87 Stuka of 1935. Constraint has been used much more recently, as for example, on the F-106 and the Tornado.

Acoustics

The cause-and-effect relationship between the shear layer and the acoustic-frequency fluctuations in the cavity has been studied extensively, but is not completely understood. Under contract to the U. S. Air Force, Heller and Bliss, of the firm of Bolt, Beranek, and Newman conducted a series of water table studies in 1972 (Ref. 16) during which it was demonstrated that the expansion of an

approaching supersonic flow into the cavity (for cavities of appropriate L/H values) would generate a pressure disturbance or wave that would travel to the downstream bulkhead, where it would be reflected. As fluid was forced from the cavity by the brief increase in pressure, the shock at the downstream edge of the cavity opening detached. When the pressure was reduced by the reflection and mass ejection, the shock again attached to the downstream edge. Meanwhile, the forward traveling reflection forced the shear layer away from the cavity until expansion at the upstream edge again took place, and the cycle began anew. A sketch illustrating the above model is shown in Fig. 7.

Further experimentation by Heller and Bliss showed that the fluctuating shear layer could be stabilized through the use of various baffles in the cavity and bulkhead edge shaping. Unfortunately, the entire effort was experimental, not at all proceeding from fundamental fluid-dynamic relationships. Consequently, no attempt was made to predict frequencies or amplitudes of the acoustic-frequency pressure oscillations in the cavity.

The flow expansion-compression-ejection model appeals to intuition, and has been proffered by many investigators. Indeed, fluctuating pressures acting on the surfaces of flat plate and cavity models have been observed by both Dix at the AEDC (Ref. 13) and Plentovich at NASA/Langley (Ref. 8). In both studies, conventional measurements of static pressures acting on surfaces in steady flow were made, with the disappointing result that repeatability was poor. A sketch of the AEDC model is shown in Fig. 8, and a typical profile of surface pressure coefficient along the centerline of the plate-cavity model with L/H = 4.5 is shown in Fig. 9, for a transonic condition. There are actually 12 profiles shown in Fig. 9, recorded at random intervals of 20 to 60 sec. Repeatability on the plate upstream of the cavity is excellent - well within the quoted statistical 95-percent confidence interval for one standard deviation of the pressure coefficient, i.e., a C_p of ± 0.01. In the cavity, the data points indicate decreasing repeatability with increasing X/L. On the plate downstream of the cavity, a convergence toward acceptable repeatability occurs. Sample profiles of both statistical mean and standard deviations are shown in Figs. 10a and 10b, respectively.

When dynamic pressure transducers are used to sense the fluctuating components of surface pressures, there is convincing correlation between the power spectra in the frequency domain at various locations and the standard deviation profile determined from the 12 repeat points. Sample spectra are shown in Fig. 11 for several locations on the plate/cavity model. Near the downstream wall in the cavity, where the one-standard-deviation profile is maximum in value, the modal and broadband amplitudes are greatest, as are the overall root-mean-square (RMS) levels. Consistently, near the upstream wall in the cavity, both low standard deviation in the static measurements and lower modal and RMS levels of fluctuating pressures are observed.

ACOUSTIC PREDICTIONS

In his 1962 RAS paper, Rossiter offers an empirical method of predicting modal frequencies,

$$f = \frac{V(m - \gamma)}{L\left(1 + \frac{\gamma - 1}{2} M^2\right)^{\frac{1}{2}}\left(\frac{V_v}{V_\infty}\right)} \quad \text{(Ref. 6).}$$

The influence of the shear layer is addressed via the vortex velocity ratio, and cavity shape in the flow direction is acknowledged through the γ term, which Rossiter presents as a function of cavity L/H. When Rossiter's values of γ are displayed graphically as a function of L/H, a mathematical relationship is difficult to propose for the purpose of interpolation and/or extrapolation, Fig. 12. For example, the cavities used by the authors in a recent set of experiments require both interpolation and extrapolation. Both first and second-order relationships were attempted, with mixed results. Interpolation via either linear or parabolic relationships yielded similar values of γ, but extrapolation beyond the range of Rossiter's results could be undertaken only subjectively (Fig. 12).

Comparison of frequency predictions with data from the recent AEDC wind tunnel experiments illustrates the limitation (Fig. 13). Tonal frequencies in a deep cavity (L/H = 4.5) are predicted quite well for modes 1 and 2 through M = 1.20, but less well for the third and higher modes. Furthermore, the predicted frequencies are underestimated for all modes at Mach numbers greater than 1.20, which happens to be the limit of Rossiter's data base. The trend of prediction quality is downward as the height of the cavity decreases (Fig. 13b, L/H = 9.0), but the issue of γ choice becomes moot for a most shallow cavity of L/H = 14.4, illustrated in Fig. 13c, for which no sharp tones are detected. Of course Rossiter's data base is also limited to L/H = 10.

Amplitude predictions represent a much more complicated situation. It may be inferred from data in the literature that the amplitude of a tone, expressed as a static pressure coefficient, is dependent on many parameters, e.g.,

$$c_p = c_p\left(\frac{tc_\infty}{L}, \bar{x}/L, L/H, W/H, M_\infty, \theta/H, \gamma\right),$$

where L, W, and H are cavity dimensions, θ is the displacement thickness of the approaching boundary layer, c_∞ is the free-stream speed of sound, t is time, x is the axial length from the leading edge of the cavity to a location in the cavity, and γ is the ratio of specific heats.

Recent AEDC data confirm no strong effect of unit Reynolds number (Fig. 14) and of Mach number (Fig. 15). However, tonal amplitude can be affected by model size, as observed by Shaw (Ref. 17). Using the authors' generic plate/cavity model (Fig. 8), filler blocks were installed which decreased the dimensions of the cavity in small steps, while maintaining the shape of the cavity, i.e. the L/H and L/W ratios were constant (W = cavity width). The same pressure transducer was used in all measurements by mounting it in the same relative location in each cavity. With the size ratio, or scale factor, represented by λ, Shaw's data can be shown in graphical form as in Fig. 16. It must be noted that the boundary layer at the leading edge of the cavity opening was constant, since the inserts were installed beginning at the downstream end of the cavity. With so many parameters interacting, development of an amplitude-prediction algorithm will be difficult, indeed. A research effort is underway at the AEDC to attempt such a correlation.

MODULATION OF THE CAVITY ACOUSTICS

A large part of the authors' series of wind tunnel experiments at the AEDC has been a study of the effectiveness of various techniques in modulating the cavity aeroacoustic environment. Two passive devices were evaluated: 1) spoiler devices mounted at or near the leading edge of the cavity, and 2) 45-deg ramp surfaces installed in the cavity at the downstream wall, illustrated in Fig. 17. Of course, cavities are usually equipped with doors, and several types were also included in the experiments (Fig. 18). Clearly, a very large data base was compiled as the many combinations of these devices were evaluated, and it will be possible to present only a small amount of the data.

Spoiler and Door Effects on Cavity Aeroacoustics

The effectiveness of a spoiler erected perpendicular to the flow at the leading edge of the cavity opening in modulating or suppressing pressure fluctuations in the cavity of an F-111 aircraft was described by Clark (Refs. 7 and 18). Although Clark identified the superior effectiveness of a combined leading-edge sawtooth spoiler and rear bulkhead ramp (Fig. 19), the internal ramp requires a cavity length that is longer than otherwise required, and is therefore not regarded with favor by the structural designer. Consequently, only spoiler-door combinations are described here. Three types of data support conclusions about the effectiveness of spoiler-door combinations, and will be discussed here.

Static Pressure Distribution

First, static pressure measurements taken along the longitudinal centerline of the cavity walls and ceiling can be used to identify the regions of high and low aerodynamic pressure acting on a body in the cavity that strongly influence the subsequent behavior of the body. In the case of a store jettisoned from a cavity, the influence of a properly designed spoiler can be extremely beneficial. For example, in Fig. 20, the influence of a sawtooth spoiler mounted at the leading edge of a cavity of L/H = 4.5, and in the presence of square-leading-edge bifold doors open to 90 deg (SBF 90) is illustrated for a transonic Mach number. Two heights of the sawtooth spoiler were used during the test, one about three times the boundary-layer height (3δ) and one approximately equal to the boundary layer (1δ). For comparison, the centerline pressure distribution of the clean cavity (no spoilers, no doors) is also shown. In this case, the store model is suspended 4.5 store diameters below the cavity opening, as if just jettisoned. Note that in the clean cavity, the pressure distribution is benign over 60 percent of the length of the cavity, but that near the rear bulkhead, the stagnation of flow causes a high pressure to build in the region of the cavity nearest the tail fins of a typical store. With the 1δ spoiler installed, there is a reduction in surface pressure to below free-stream static throughout the cavity, and a significant reduction in the stagnation region. This influence is made stronger when the 3δ spoiler is installed.

Store Loads

Spoiler influence is also illustrated in Fig. 21 using the second type of data, store aerodynamic loads. Store loads were measured using a strain-gage balance inside the sting-mounted store model. The important pitching moment is almost neutral as the store leaves the clean cavity. When the 1δ spoiler is installed, the desirable nose-down pitch is improved, and with the 3δ spoiler, dramatically improved. Unfortunately, the benefit does not remain as Mach number increases, and at low supersonic conditions, the influences of a spoiler are indistinguishable from the clean cavity (Fig. 22).

That the spoiler influence is not so much dependent on the type of doors but rather on the leading edge shape can be seen in Figure 23. The 3δ sawtooth spoiler was mounted on the L/H = 90 cavity with three different doors: square leading-edge single fold, or "cafe", doors open to 90 deg (SC 90); the SBF 90 doors mentioned above; and tapered-leading-edge cafe doors open to 90 deg (TC 90). The spoiler effect is the same for the square leading-edge doors, but significantly less effective for the tapered leading-edge doors until the low supersonic regime, where the shock structures emanating from the doors dominate the store loads. These loads are summarized as a function of Mach Number in Fig. 23b.

While the qualitative effects of spoilers and doors on surface pressures and store loads are quite understandable from the aerodynamist's intuition, what is not available is an easy-to-use method of predicting the magnitude of the effects. CFD techniques can be brought to bear on the problem, but the complex mesh that must be defined, with separate grids for each component, drive computing costs to exorbitant levels.

Acoustic Environment

The third measure of spoiler/door influence is the acoustic environment of the cavity. Advances in transducer technology have reduced the differences between "static" and "unsteady" pressure-measuring techniques to largely a matter of where the transducer is located. In most wind tunnel models, internal volume is severely limited, so transducers are usually located outside the model and connected to the orifice on the model via small tubes. The output voltage of the transducer is sampled tens of thousands of times each second for a period of time considered adequate to determine a valid mean value of the pressure at the orifice. Unsteady, or fluctuating pressures are sensed in much the same way, except that contemporary transducers are self-contained in a relatively small package that is mounted directly in the surface of the model.

During the AEDC cavity tests, a total of 45 transducers were mounted in the plate/cavity model, most serving as alternates in case of loss of signal from an adjacent transducer. Along the longitudinal centerline of the cavity, the transducers were mounted with a spacing of approximately 0.9-in. center-to-center (Fig. 24). The output of each transducer was recorded 10,000 times each second for 5 secs. Data were reduced via FFT techniques using 1,024-point ensembles, so that the bandwidth of the analysis was 9.77 Hz.

As a sample of the data, the effectiveness of a spoiler in modulating the tonal amplitudes sensed by transducer number 16 at the rear bulkhead of a deep cavity (L/H = 4.5) is illustrated in Fig. 25 for a transonic condition. (Spoiler effectiveness in a shallow cavity, say L/H = 9.0, at the same condition is not as noticeable as for the deep cavity since the tones diminish as L/H is decreased.) The noise-reduction effectiveness of the coarse sawtooth and the fine sawtooth 3δ spoilers is compared in Fig. 25b. The ordinate, $\Delta P_{RMS}/q_\infty$ represents the difference in the overall SPL (coverted to an rms pressure and normalized by free-stream dynamic pressure) at tranducer K16 between a cavity with the coarse sawtooth 3δ spoiler and a cavity with the fine sawtooth 3δ spoiler. Although the noise reduction using the coarse sawtooth is beneficial at subsonic conditions, their is no clear advantage of coarse over tine sawtooth in the supersonic regime, where the presence of shock structures overwhelm turbulence.

The authors' AFATL/AEDC data base contains over a thousand spectra representing many combinations of spoilers, doors, and ramps. Clearly it would be impossible in a survey paper to discuss more than a few cases. The data discussed herein tend to substantiate results reported by others. What is new is the compilation into one data base of experimental data defining the many interactions in the flow field caused by the presence of multiple physical features.

CFD CALCULATIONS

Using a CRAY XMP computer, Suhs at the AEDC has predicted flow fields in empty cavities (Ref. 9). His technique has been to use a time-accurate full Navier-Stokes solver with viscosity effects confined to a thin layer adjacent to the surfaces. A stretched Cartesian grid was also used, increasing the density of grid cells close to the model surfaces, and increasing cell size in regions well away from the walls (Fig. 26). Good agreement with measurements has been obtained (Fig. 27), but solutions for an empty cavity have required 10 to 20 hours of computation to complete. Sketches of the mass flux through the plane of a cavity opening are shown in Fig. 28. The sketches were recorded at 0.4 of a time characteristic (0.00085 sec) intervals (see Ref. 9 for more details). At present, grids for a store model and a sting are being added, with the concomitant increase in calculation time - upwards of 40 hours of CPU time. Current flow models include a modified Baldwin-Lomax turbulence model. Further discussion of CFD results will be left to other authors.

SCHLIEREN EVIDENCE - SUPERSONIC REGIME

During a series of tests at supersonic conditions, some schlieren movies were recorded at a rate of 4,000 frames/sec. Visual evidence of laminar-to-turbulent-to-laminar behavior was observed as the boundary-layer flow moved downstream from over the plate to over the cavity (Fig. 29). Although this behavior was not expected, the effect on cavity pressure distributions and acoustic tonal amplitudes was not detected. In fact, at a constant unit Reynolds number of approximately 3×10^6 per foot, the overall (rms) level at transducer 16 tended to peak in the transonic regime and decrease as Mach number increased. Furthermore, tonal amplitudes abate as Mach number increases, so that in the supersonic regime only broadband noise is evident (Fig. 30).

CONCLUDING REMARKS

Cavity aeroacoustics - a challenge of recurring practical interest for the past 60 years - has yielded stubbornly to researchers to date. The engineering method of Rossiter for predicting modal frequencies to be expected in certain simple rectangular cavities exposed to grazing transonic flow provides adequate, if not perfect, guidance to the designer. Beyond the limits of Rossiter's data base in cavity geometry and flow velocity, however, the method falters. Although there is at least a

possibility of predicting modal frequencies, there is unfortunately no easily applied method of predicting modal amplitudes. Not only are wind tunnel tests conducted at incorrect Reynolds numbers, but scale effects on acoustic leve's have also been observed. CFD solutions are being reported, but the complex grids and turbulence models required represent computation-intensive demands on expensive Class VI computing machines. Efforts underway at the AEDC to organize and correlate existing data could produce at least a first-order amplitude-prediction technique within a year.

In the meantime, a large data base of cavity pressure measurements - both static and unsteady - and store loads has been assembled at the AEDC under the sponsorship of AFATL. From these data, some helpful general trends have been observed, to wit: 1) spoilers mounted at the leading edge of a cavity opening are effective in suppressing aeroacoustic phenomena only in the subsonic-transonic regime, losing effectiveness at supersonic conditions, 2) the effectiveness of a spoiler is independent of square leading-edge door type (single-fold or bifold), but the effectiveness is weakened by the strong flow field around a tapered leading-edge door, especially as velocity increases, and 3) the overall (rms) acoustic amplitude in a cavity is not a function of Reynolds' number.

Fortunately, safe separation of stores jettisoned from a cavity can be assured if sufficient outward velocity and pitch rate are imparted to the store. In other words, the shear layer can be defeated if the residence time of the store passing through it is minimized, so that inertia dominates. Whether the structural and functional integrity of the bodies in the cavity can be assured after the imposition of the necessary forces and acceleration is quite another question, as is the question of survival of exposure to acoustic tones on the order of 170 db. These questions are beyond the scope of this paper.

BIBLIOGRAPHY

1. Krishnamurty, K., "Acoustic Radiation from Two-Dimensional Rectangular Cutouts in Aerodynamic Surfaces," NACA TN 3487, August 1955.

2. Tam, C.K.W. and Block, P. J. W., "On the Tones and Pressure Oscillations Induced by Flow Over Rectangular Cavities," Journal of Fluid Mechanics, Vol. 89, 1978, pp. 373-399.

3. Bilani, A. J. and Covert, E. E., "Estimates of Possible Excitation Frequencies for Shallow Cavities," AIAA Journal, Vol. 11, 1953, pp. 347-351.

4. Covert, Eugene E., "An Approximate Calculation of the Onset Velocity of Cavity Oscillations," AIAA Journal, Vol. 8, No. 12, December 1970, pp. 2189-2194.

5. Stallings, Robert L., Jr. and Wilcox, Floyd J., Jr., "Experimental Cavity Pressure Distributions at Supersonic Speeds," NASA Technical Paper 2683, June 1987.

6. Rossiter, J. E., "Wind Tunnel Experiments on the Flow Over Rectangular Cavities at Subsonic and Transonic Speeds," Ministry of Aviation, Aeronautical Research Council Reports and Memoranda, R&M No. 3438, October 1964.

7. Clark, Rodney L., "Weapons Bay Turbulence Reduction Techniques," AFFDL-TM-75-147-FXM, December 1975.

8. Plentovich, E. B., "Study of Three-Dimensional Cavity Flow at Transonic Speeds," AIAA Paper No. AIAA-88-2032, presented at the AIAA 15th Aerodynamic Testing Conference, San Diego, California, May 18-20, 1988.

9. Suhs, N. E., "Computations of Three-Dimensional Cavity Flow at Subsonic and Supersonic Mach Numbers," AIAA Paper No. AIAA-87-1208, presented at the AIAA 19th Fluid Dynamics, Plasma Dynamics, and Lasers Conference, June 8-10, 1987, Honolulu, Hawaii.

10. Rizzetta, Donald P., "Numerical Simulation of Supersonic Flow Over a Three-Dimensional Cavity," AIAA Paper No. AIAA-87-1288, presented at the AIAA 19th Fluid Dynamics, Plasma Dynamics, and Lasers Conference, June 8-10, 1987, Honolulu, Hawaii.

11. Baysal, O., Srinivasan, S., and Stallings, R. L., Jr., "Unsteady Viscous Calculations of Supersonic Flows Past Deep and Shallow Three-Dimensional Cavities," AIAA Paper No. AIAA-88-0101, presented at the AIAA 26th Aerospace Sciences Meeting, January 11-14, 1988, Reno, Nevada.

12. Stallings, R. L., Jr., "Store Separation from Cavities at Supersonic Flight Speeds," Journal of Spacecraft, Vol. 20, No. 2, March-April 1983, pp. 129-132.

13. Dix, R. E., "On Simulation Techniques for the Separation of Stores from Internal Installations," SAE Technical Paper No. 871799, presented at the SAE Aerospace Technology Conference and Exposition, Long Beach, California, October 5-8, 1987.

14. Carman, J. B., Jr., Hill, D. W., Jr., and Christopher, J. P., "Store Separation Testing Techniques of the Arnold Engineering Development Center, Volume II, Description of Captive Trajectory Store Separation Testing in the Aerodynamic Wind Tunnel (4T)," AEDC-TR-79-1 (AD-A087561), June 1980.

15. Keen, K. Scott, "New Approaches to Computational Aircraft/Store Weapons Integration," AIAA Paper No. AIAA-90-0274, presented at the 28th Aerospace Sciences Meeting, January 8-11, 1990, Reno, Nevada.

16. Heller, H. H. and Bliss, D. B., "Aerodynamically-Induced Pressure Oscillations in Cavities - Physical Mechanisms and Suppression Techniques," AFFDL-TR-74-133 (AD-B002701), February 1975.

17. Shaw, L. L., "Scale Effect on the Flow-Induced Acoustic Environment in Cavities - Wind Tunnel Test Results," WRDC-TM-89-159-FIBG, February 1989.

18. Clark, Rodney L, "Evaluation of F-111 Weapon Bay Aero-acoustic and Weapon Separation Improvement Techniques," AFFDL-TR-79-3003, February 1979.

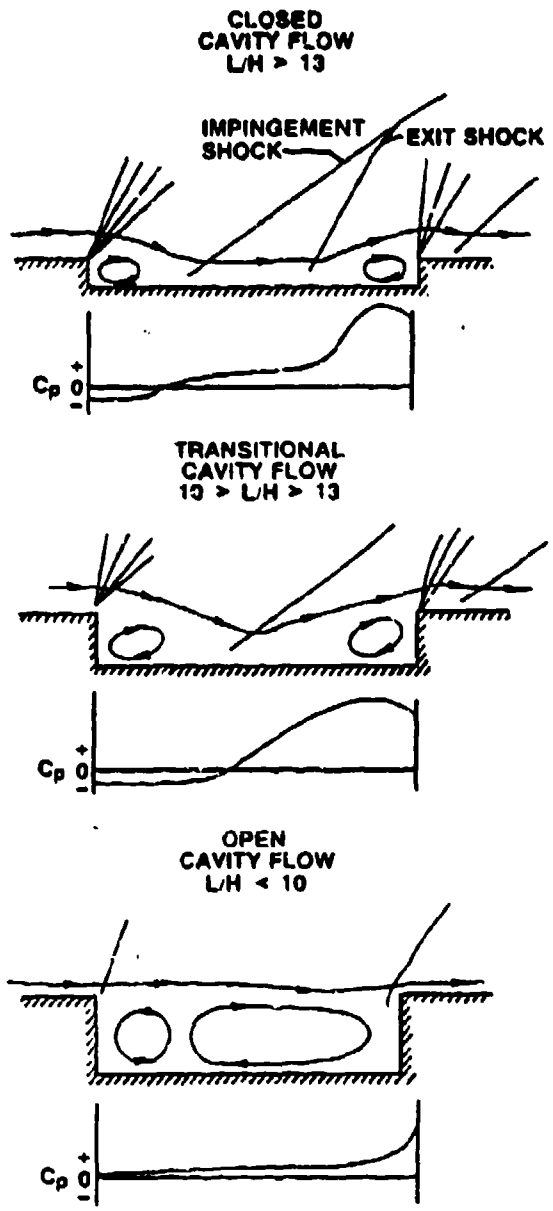

Fig. 1. Cavity flow field models (Ref. 5).

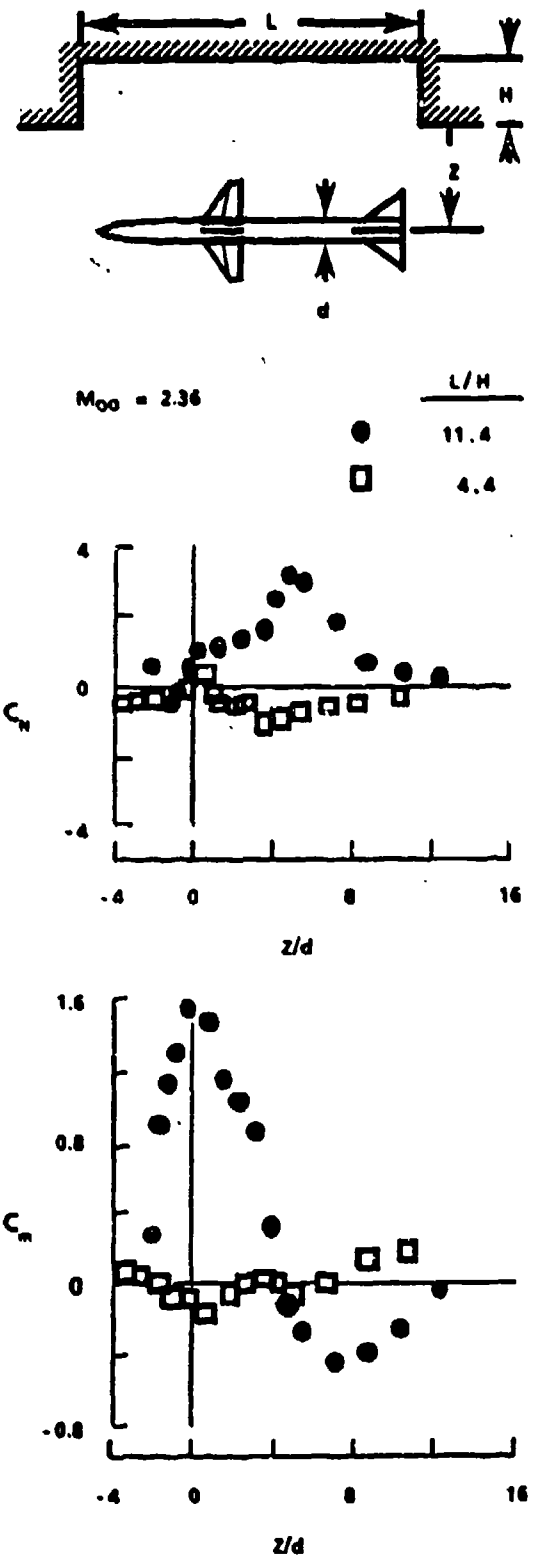

Fig. 2. Gradients in store loads through a shear layer (Ref. 12).

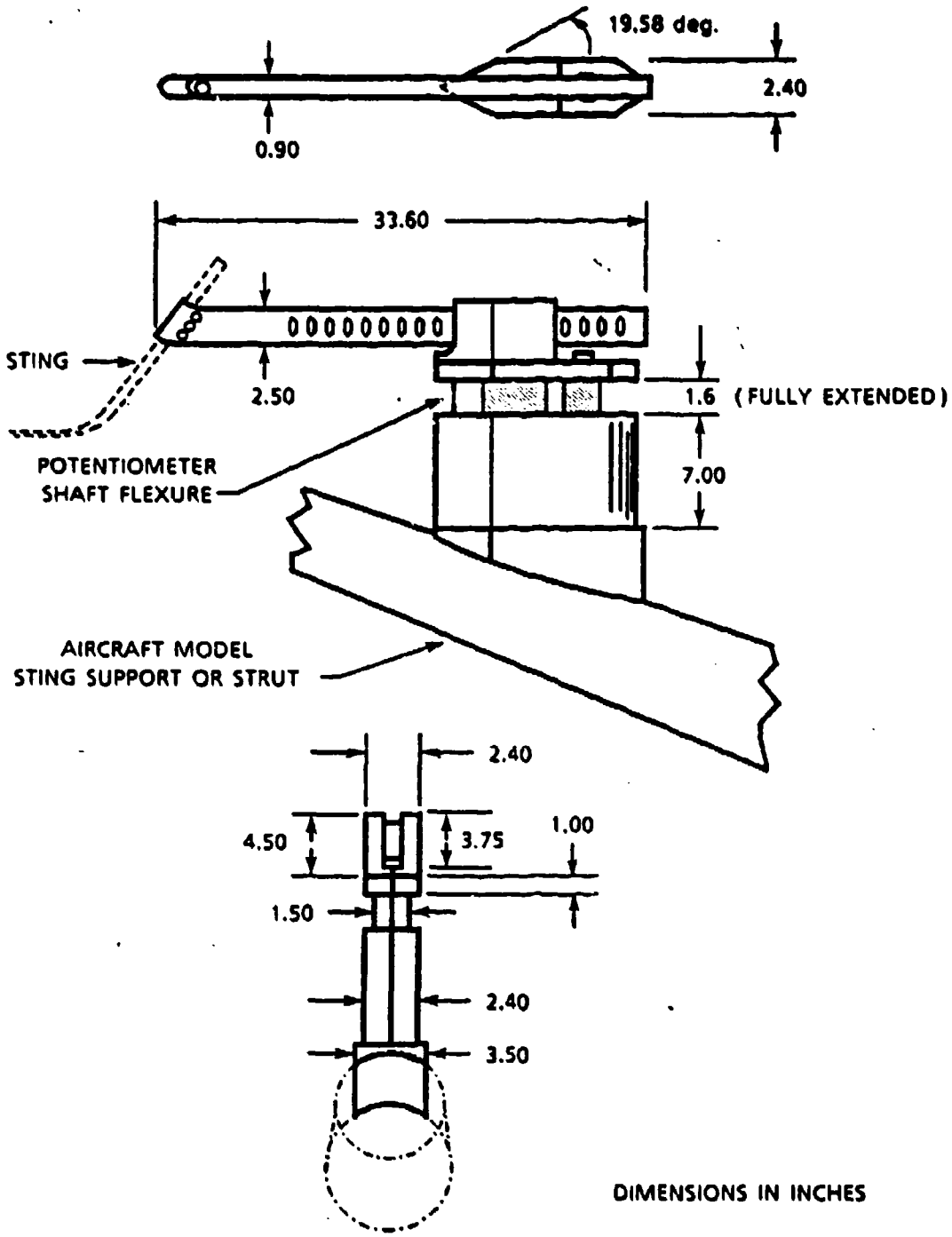

Fig. 3. Sketch of the single-axis translating sting support (Z-Rig).

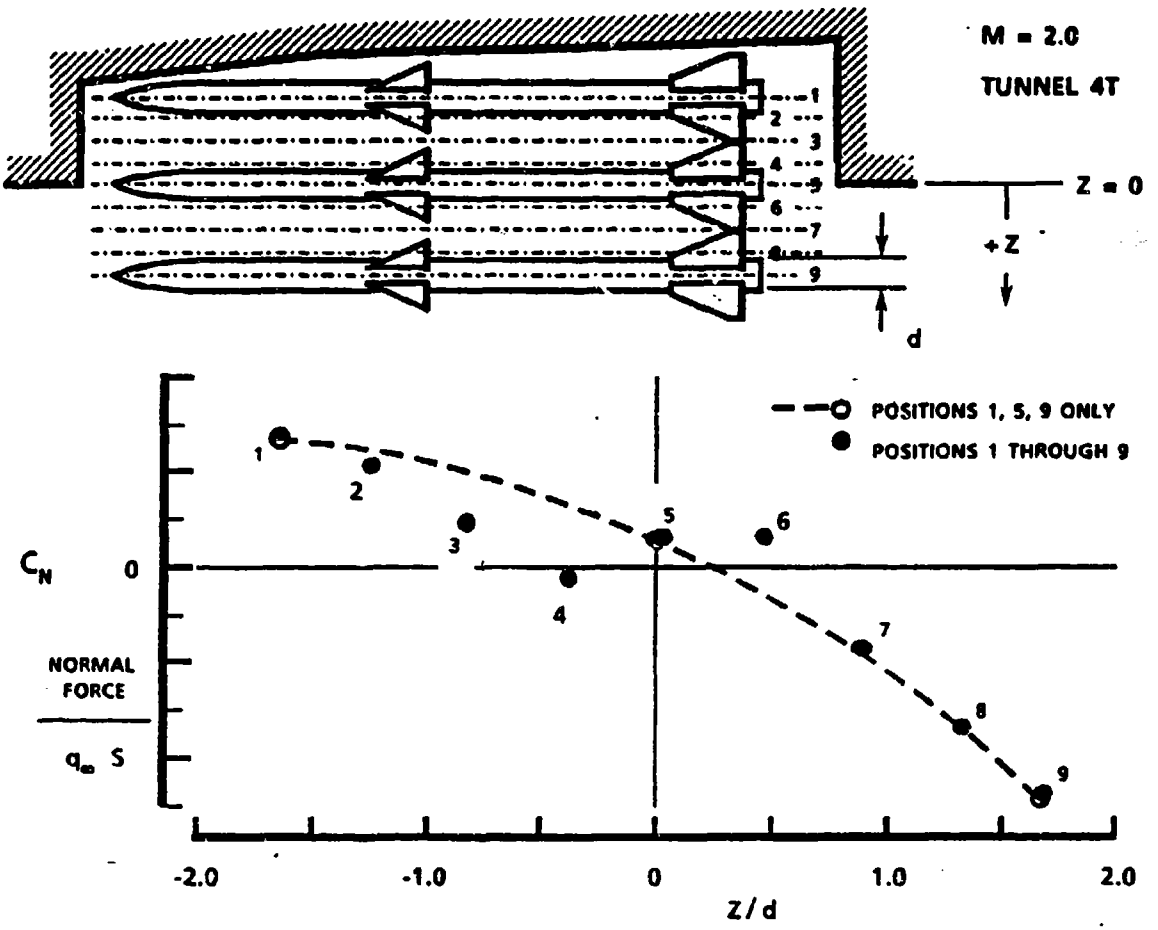

Fig. 4. Incomplete loads from limited data in a shear layer.

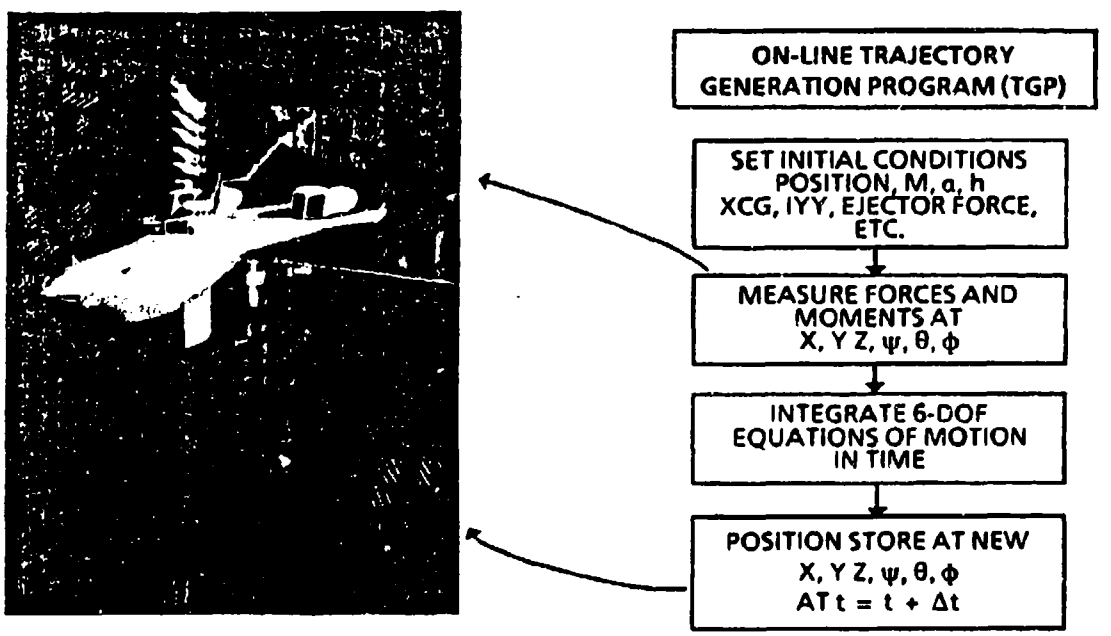

Fig. 5. The two-sting Captive Trajectory System (CTS) system at the AEDC.

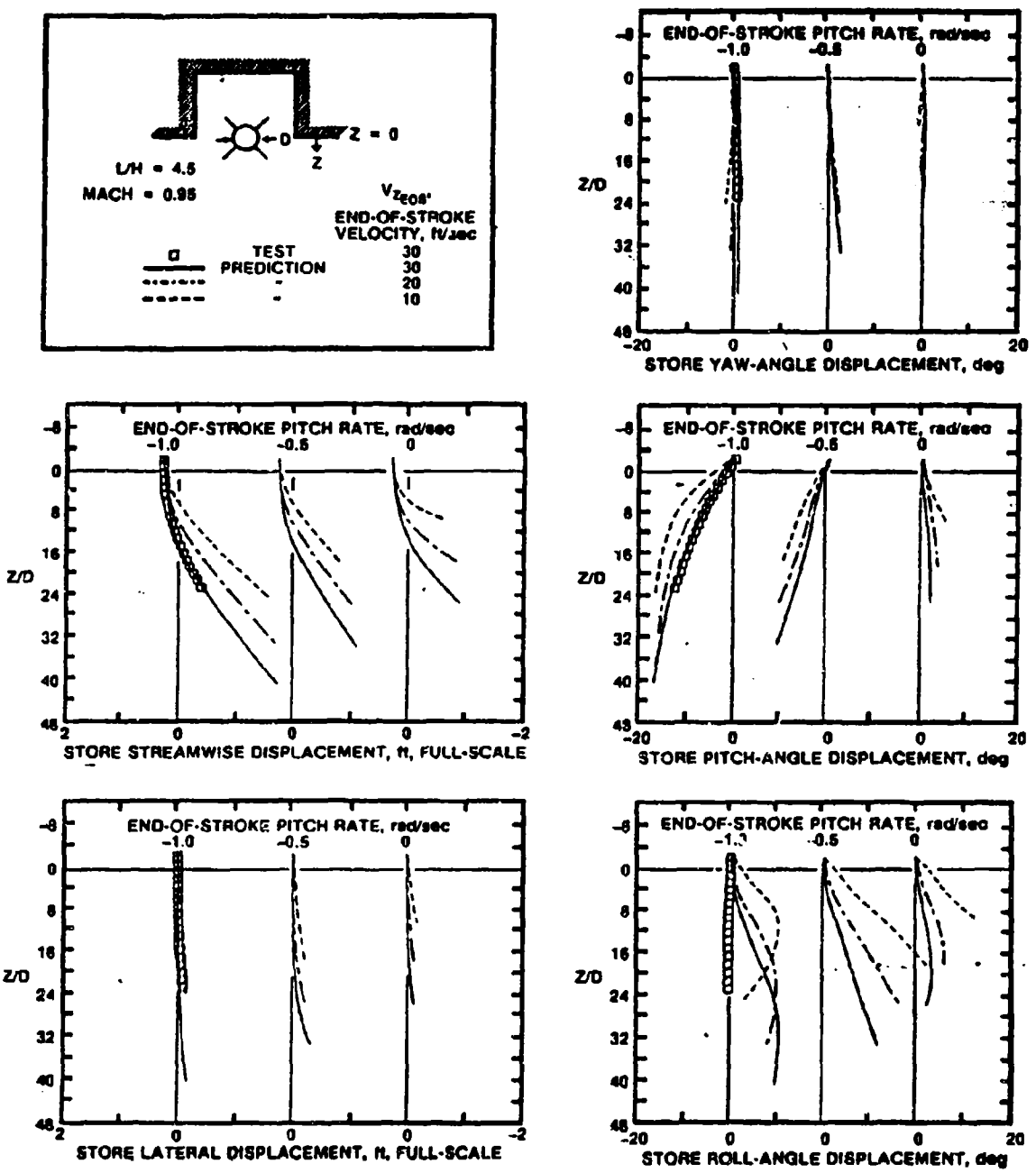

Fig. 6. Examples of calculated separation trajectories for a store ejected from a generic cavity.

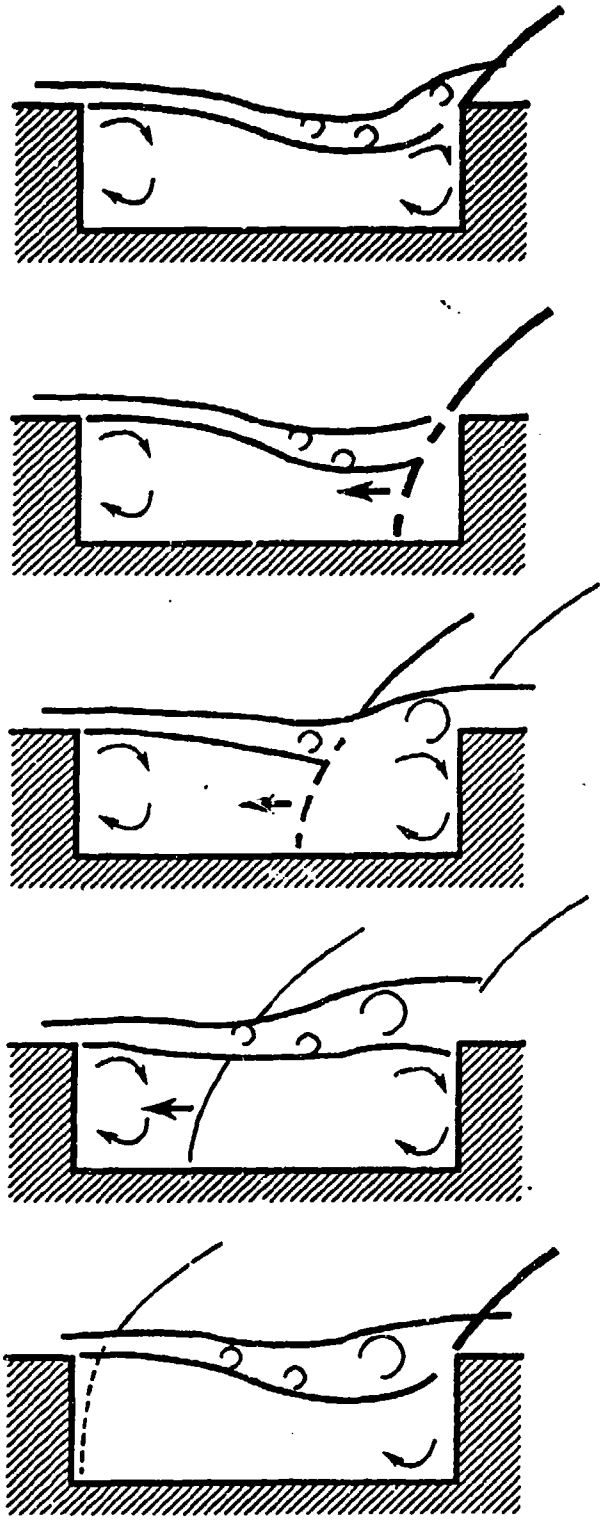

Fig. 7. Qualitative sketch of the flow-development over a cavity (from water-table experiments).

DIMENSIONS IN INCHES

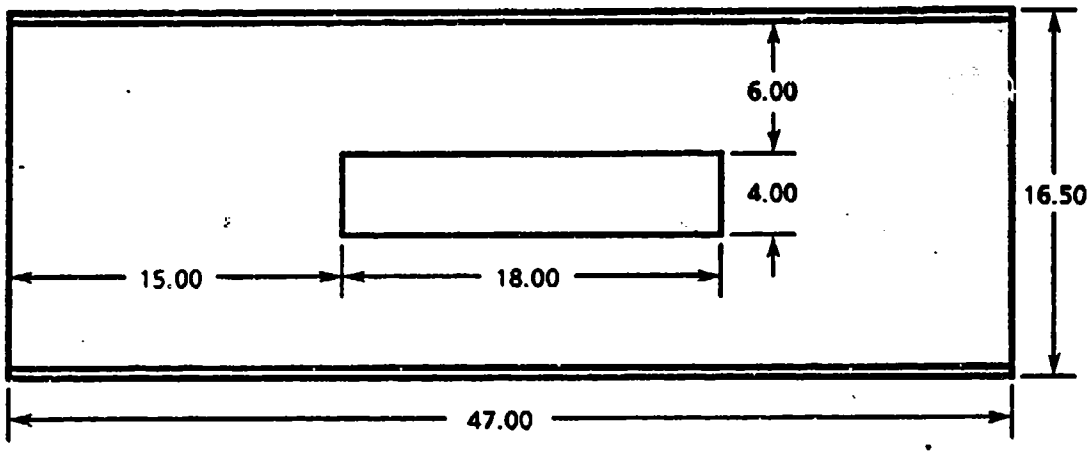

TOP VIEW (AS MOUNTED IN WIND TUNNEL) OF PLATE/CAVITY MODEL

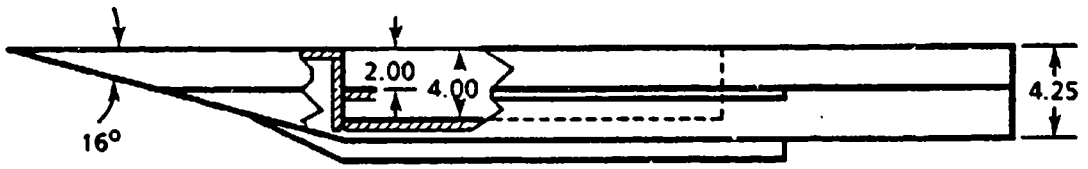

SIDE VIEW OF PLATE/CAVITY MODEL

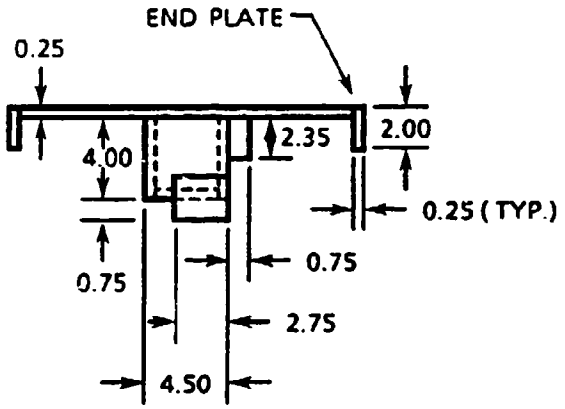

FRONT VIEW OF PLATE/CAVITY MODEL
LOOKING DOWNSTREAM

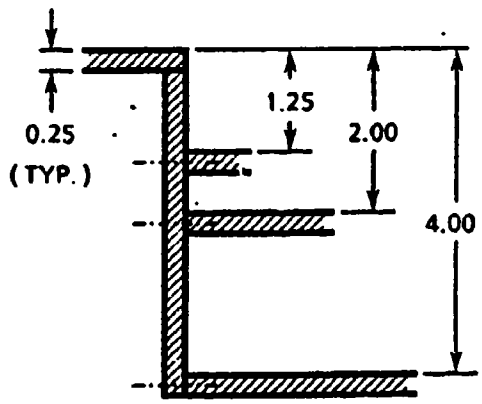

SECTION THROUGH CAVITY
SHOWING ADJUSTABLE CEILING

Fig. 8. Generic flat-plate/cavity model, mounted inverted in the wind tunnel.

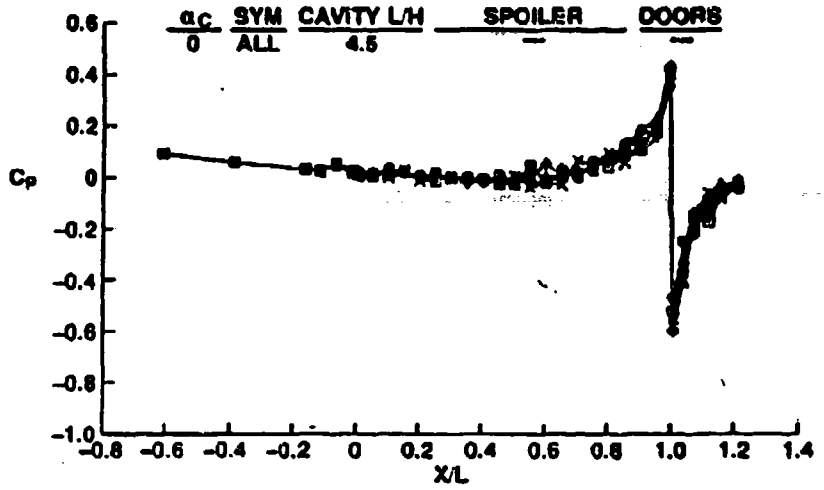

Fig. 9. Variation in centerline surface pressures acting on a generic flat-plate cavity.

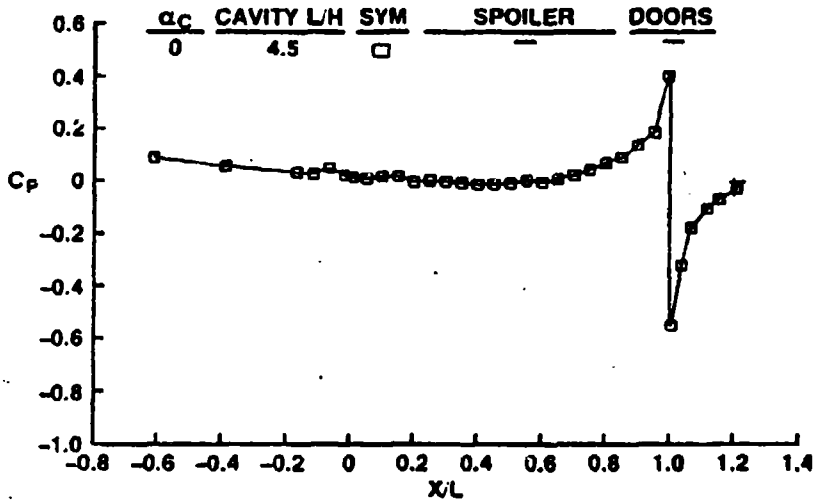

a. Mean pressure profile

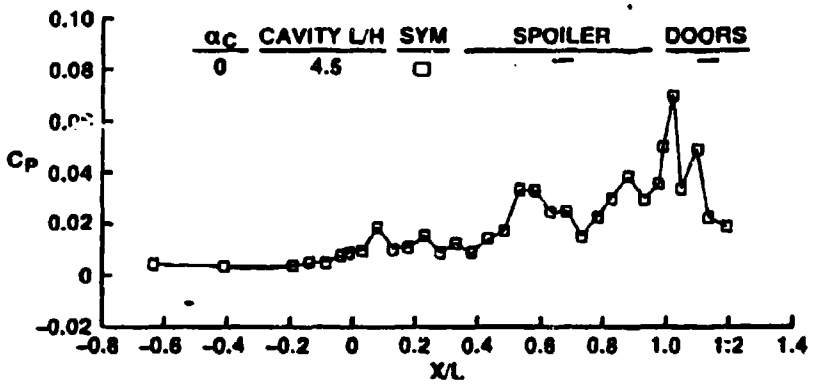

b. Profile of one standard deviation

Fig. 10. Statistical profiles for twelve repeated measurements of plate/cavity surface pressure.

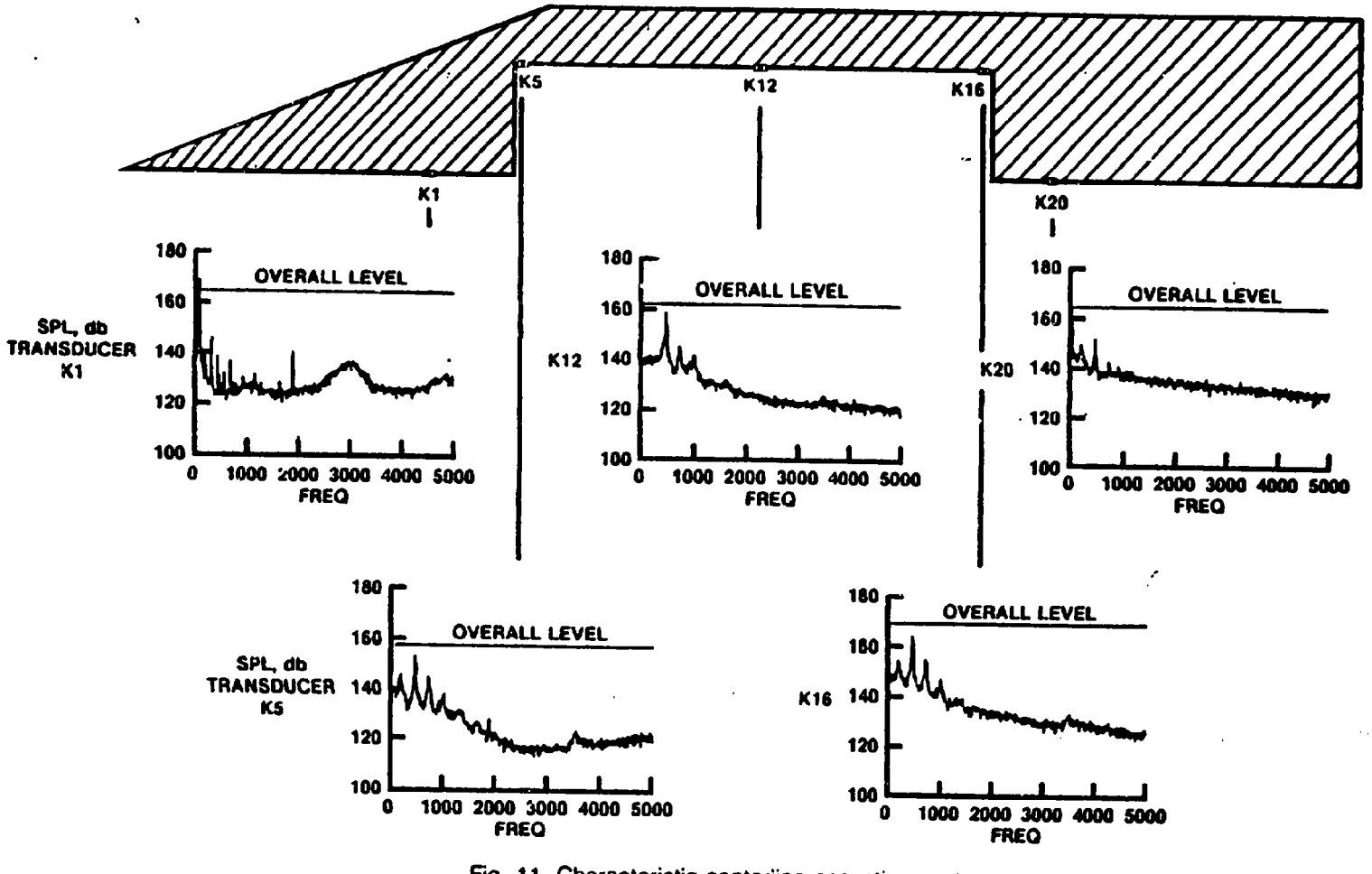

Fig. 11. Characteristic centerline acoustic spectra.

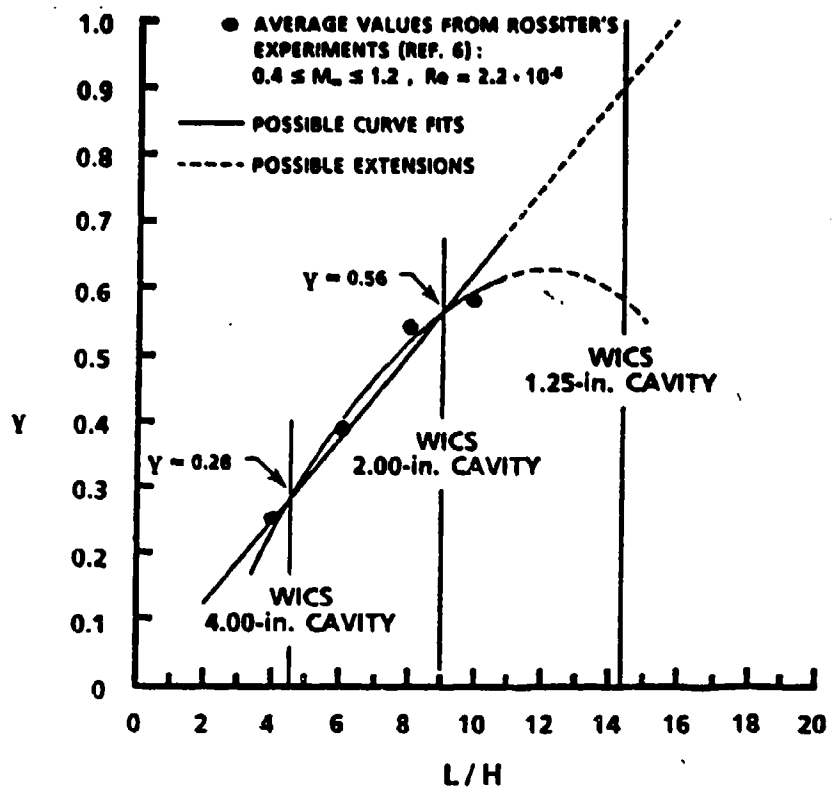

Fig. 12. Rossiter's γ term (Ref. 6).

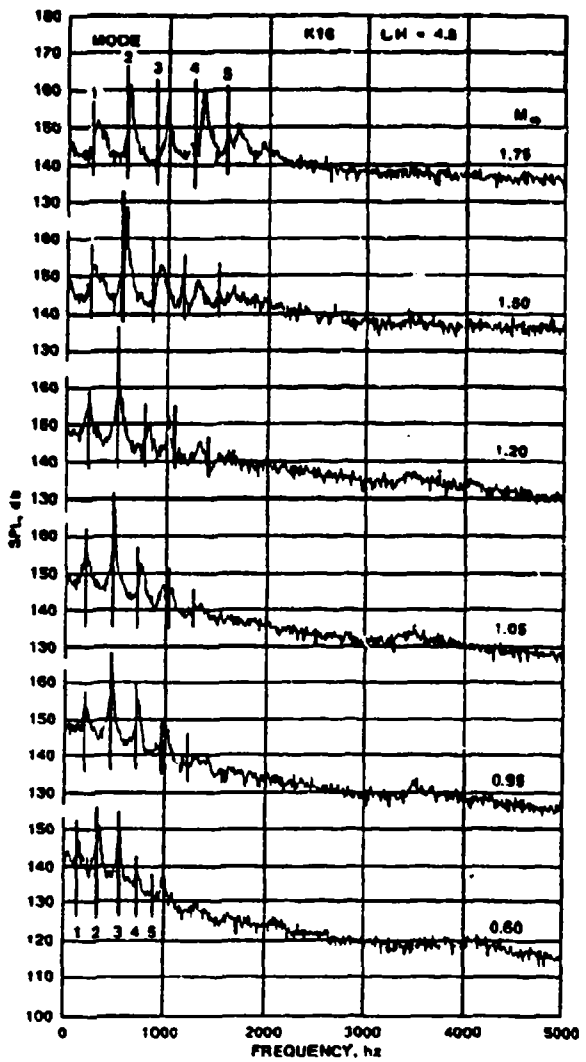

a. Cavity L/H = 4.5, transducer K16

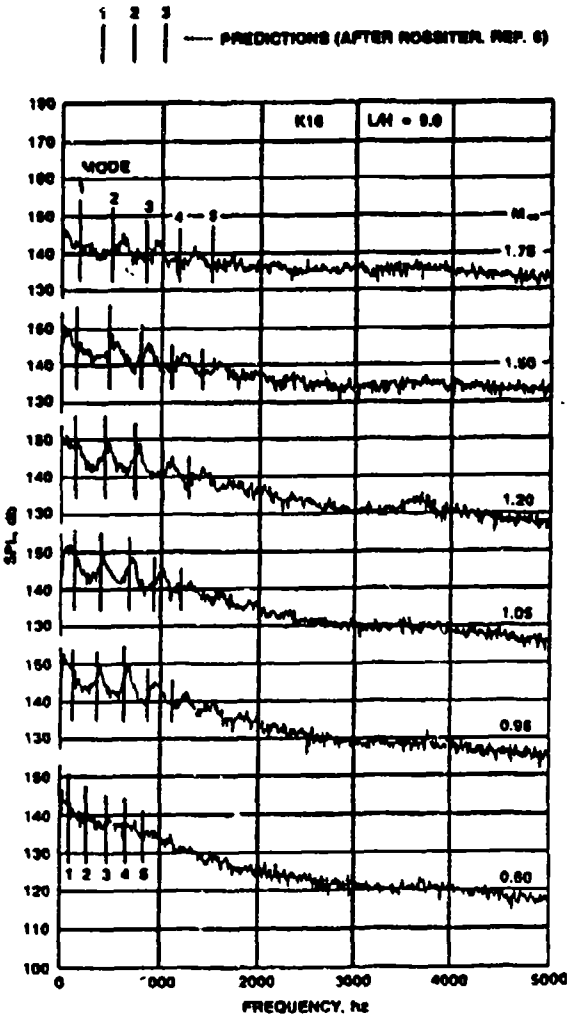

b. Cavity L/H = 9.0, transducer K16

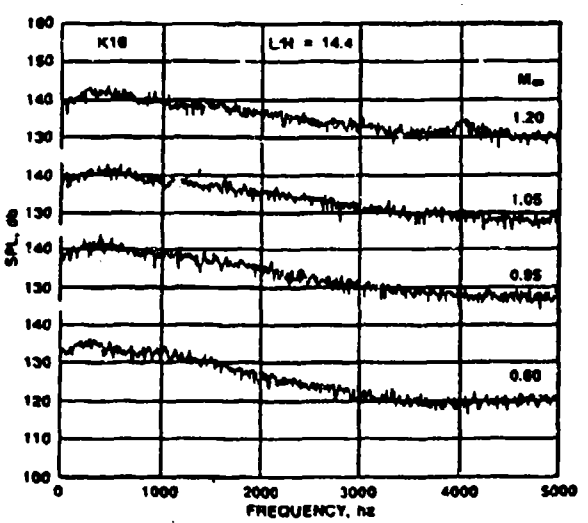

c. Cavity L/H = 4.5, transducer K16

Fig. 13. Comparison of measured and predicted modal frequencies.

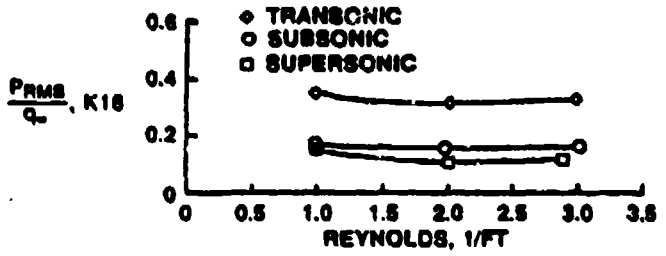

Fig. 14. Reynolds number effect on overall sound pressure level.

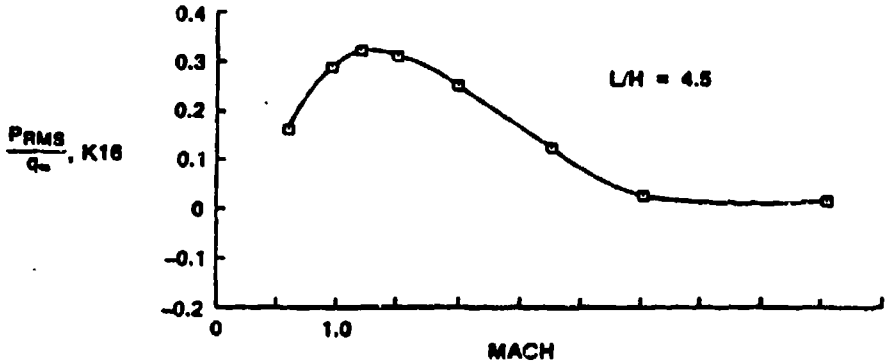

Fig. 15. Mach number effect on overall sound pressure level.

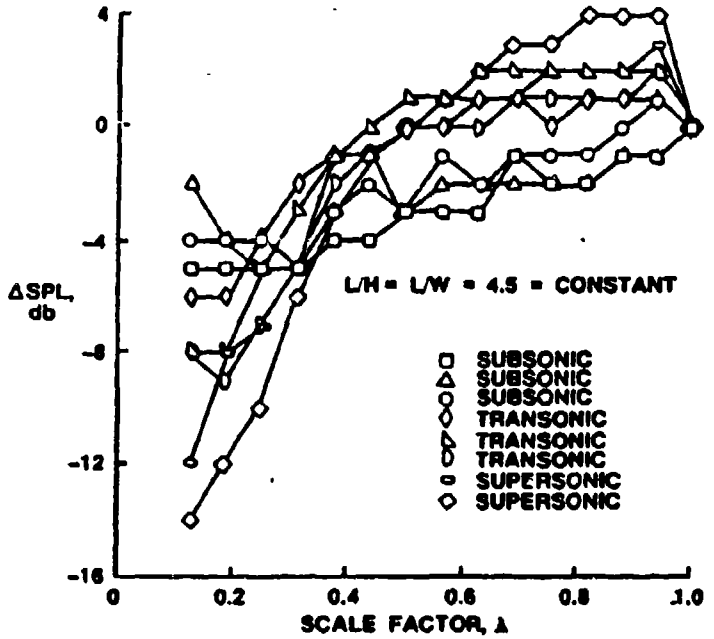

Fig. 16. Scale effect on overall sound pressure level.

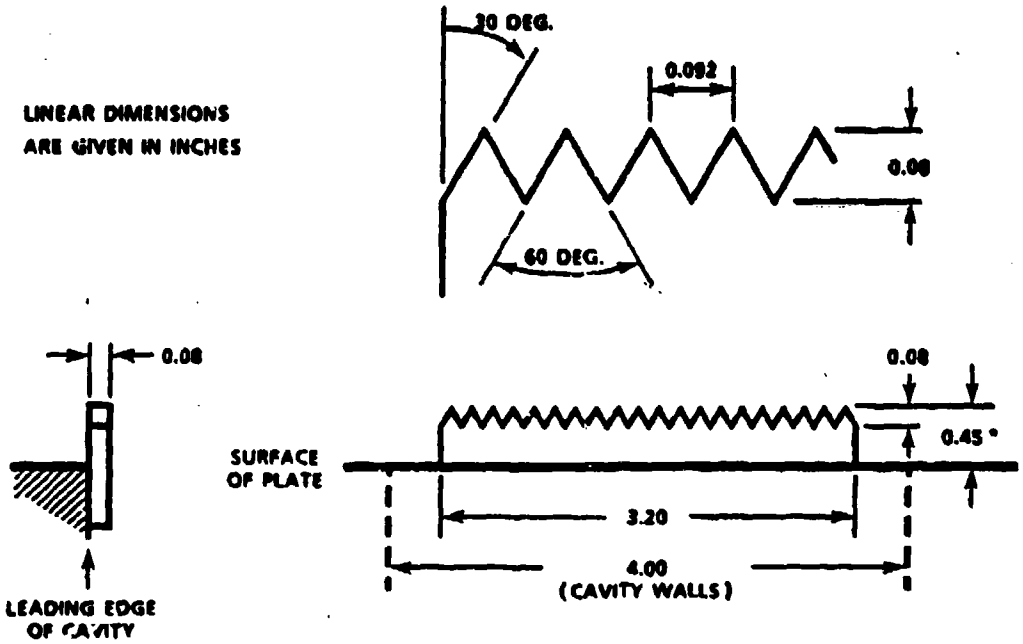

0.45-IN.* SAWTOOTH SPOILER, FINE PITCH

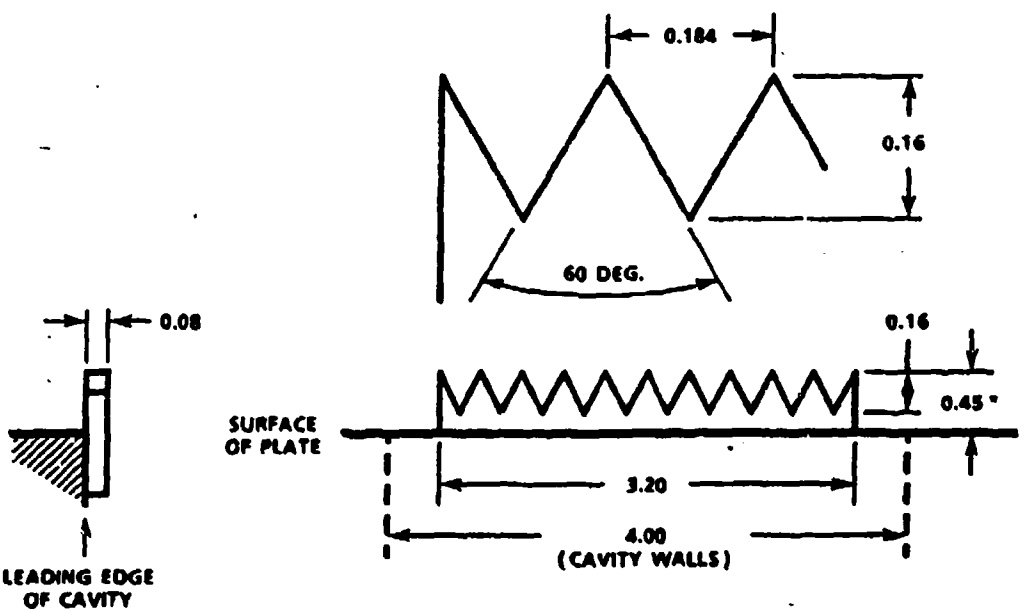

0.45-IN.* SAWTOOTH SPOILER, COURSE PITCH

* 0.45-in. Spoiler shown; 0.15-in. and 0.30-in. differ in total height, not in sawtooth design

a. Sawtooth spoilers

Figure 17. Spoiler and ramp model sketches.

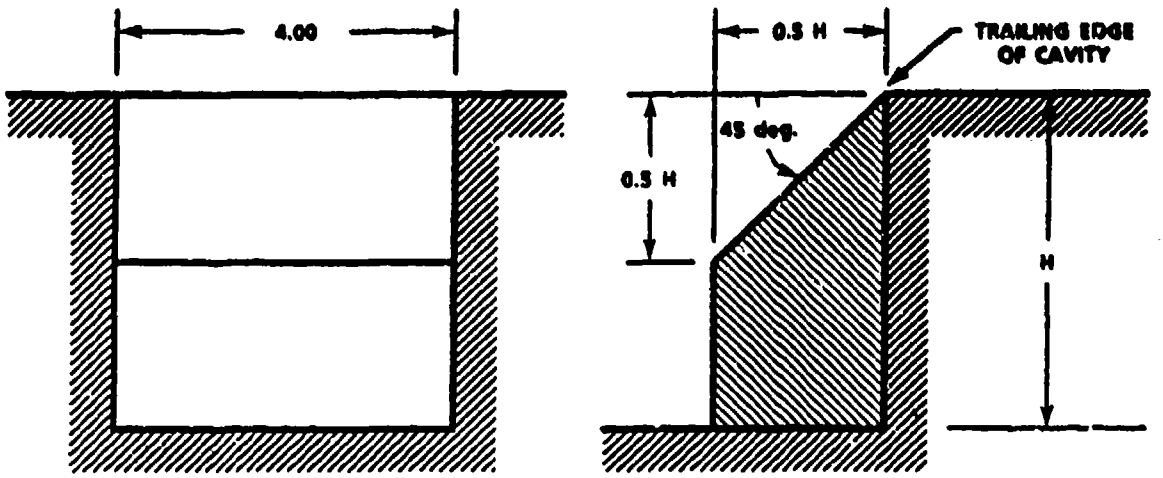

45-DEGREE SOLID RAMP

LINEAR DIMENSIONS ARE GIVEN IN INCHES

NOTE: H = 4.00, 2.00, OR 1.25 in.

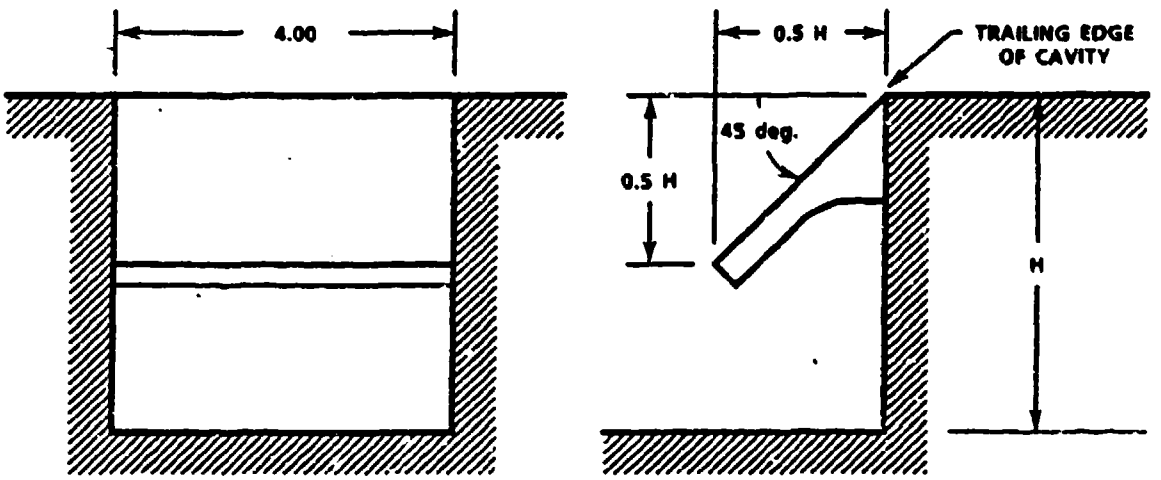

45-DEGREE SIMULATED HINGED RAMP

b. Ramp models
Figure 17. Concluded.

LINEAR DIMENSIONS ARE GIVEN IN INCHES

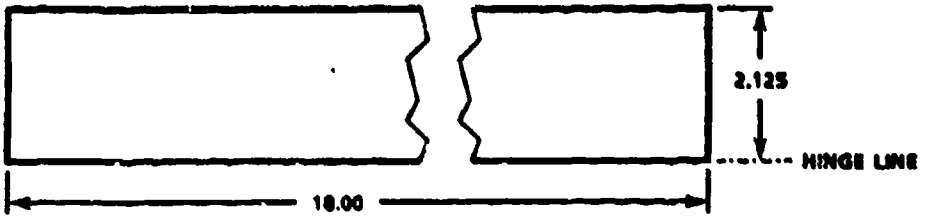

SQUARE LEADING EDGE (SC)

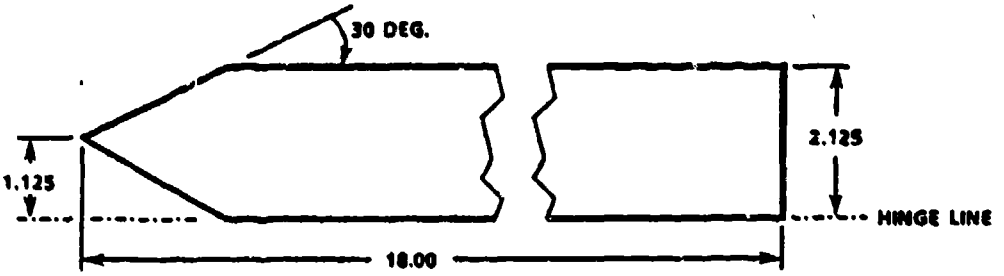

TAPERED LEADING EDGE (TC)

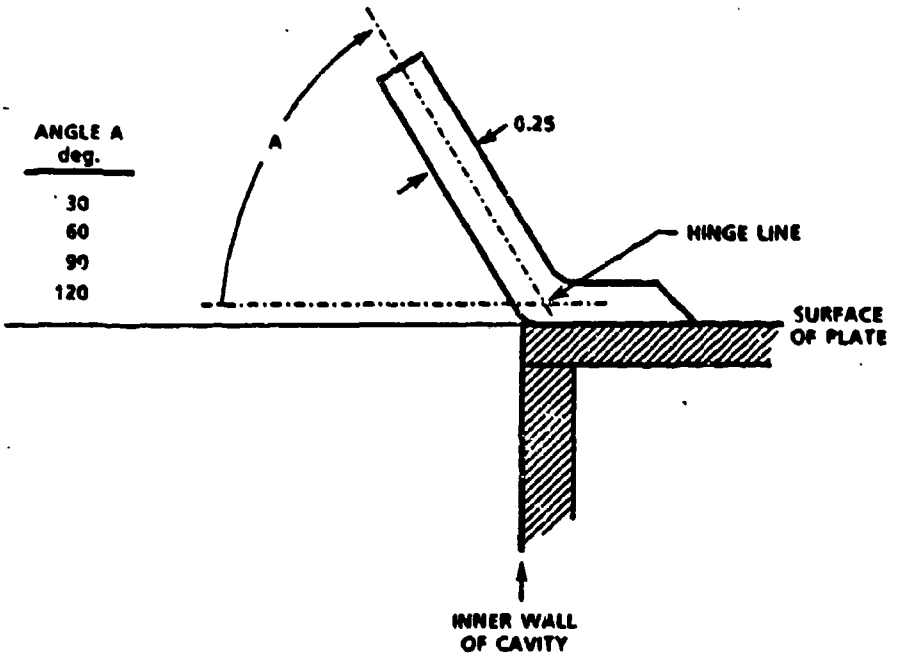

a. Cafe doors

Figure 18. Cavity door model sketches.

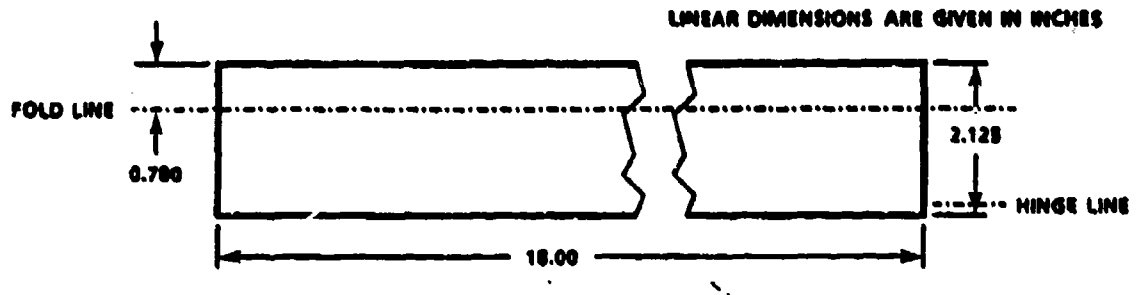

SQUARE LEADING EDGE (SBF)

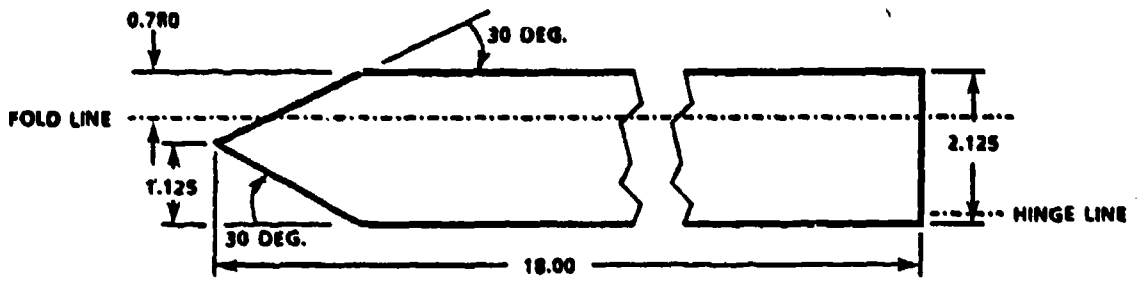

TAPERED LEADING EDGE (TBF)

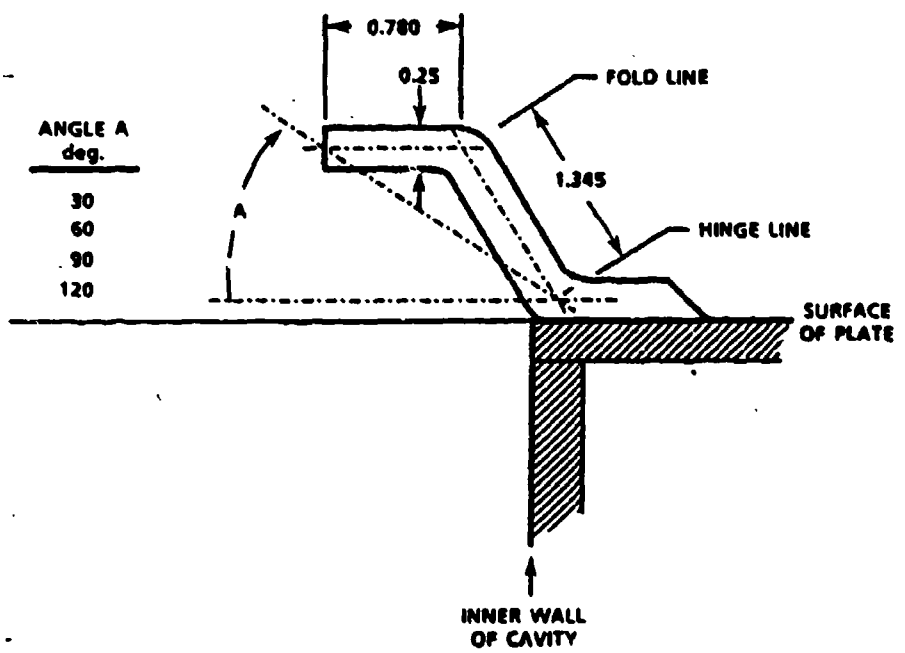

b. Bi-fold doors
Figure 18. Concluded.

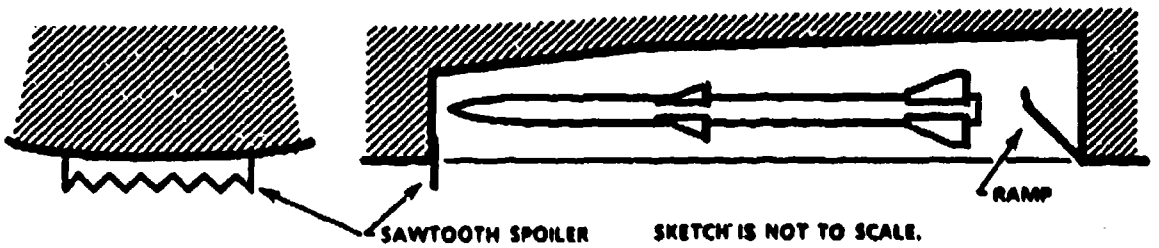

Fig. 19. Sketch of combined sawtooth spoiler and rear bulkhead ramp (Ref. 18).

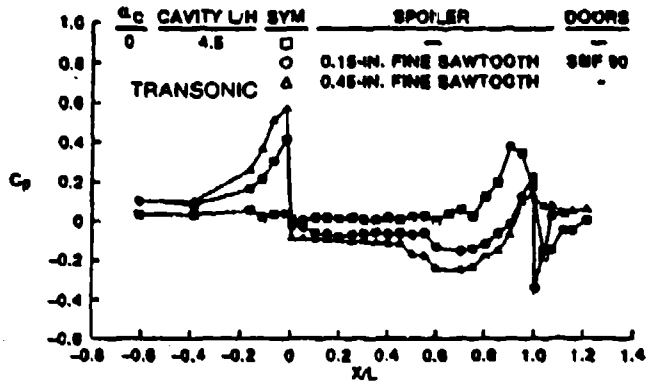

Fig. 20. Centerline surface pressure profile with a store model suspened 4.5 diameters outside the cavity opening.

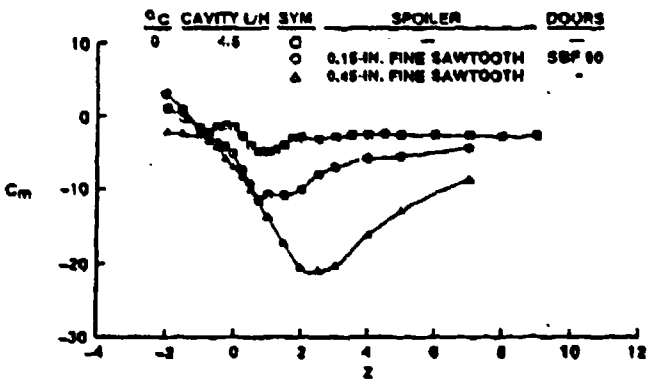

Fig. 21. Pitching moment acting on a store model along a constant-attitude Z-axis translation, transonic condition.

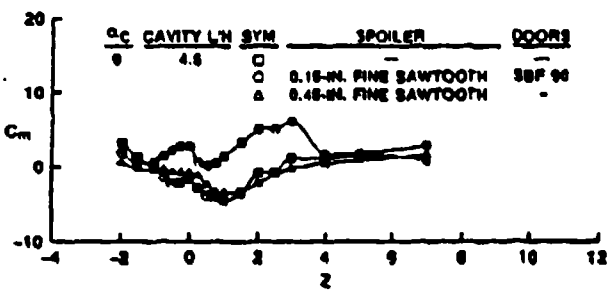

Fig. 22. Pitching moment acting on a store model along a constant-attitude Z-axis translation, supersonic condition.

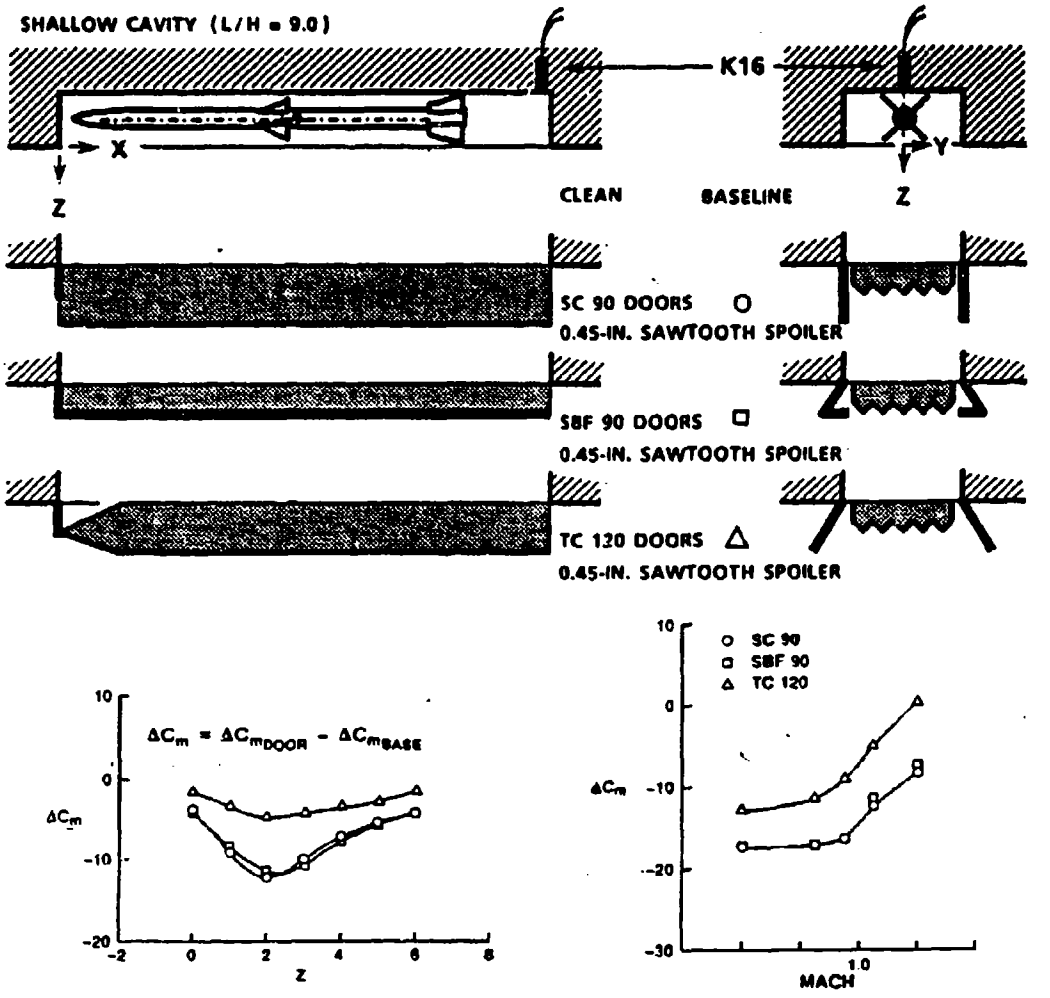

a. Transonic condition

b. Variation with Mach number at Z = 2 ft (full scale)

Fig. 23. Difference in pitching moment acting on a store model along a Z-axis translation out of a cavity with a 36 sawtooth spoiler and various styles of doors.

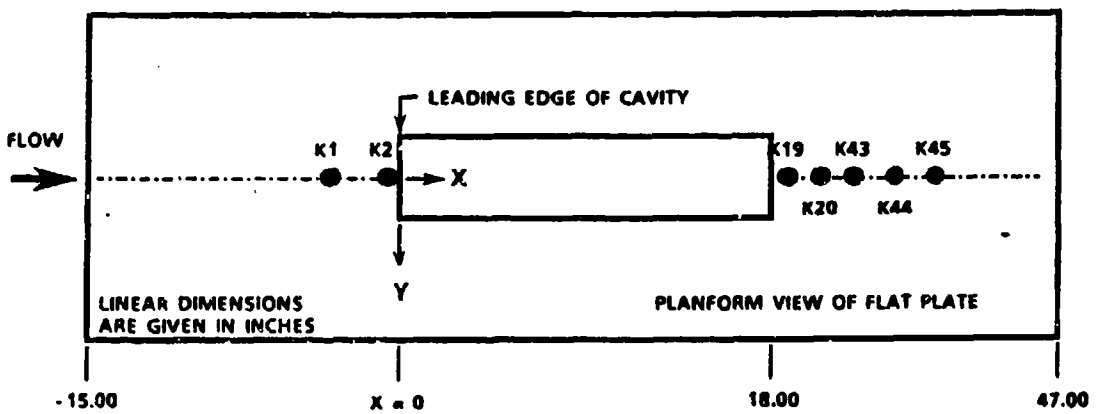

a. Location of pressure transducers on the flat plate

Figure 24. Pressure transducer locations.

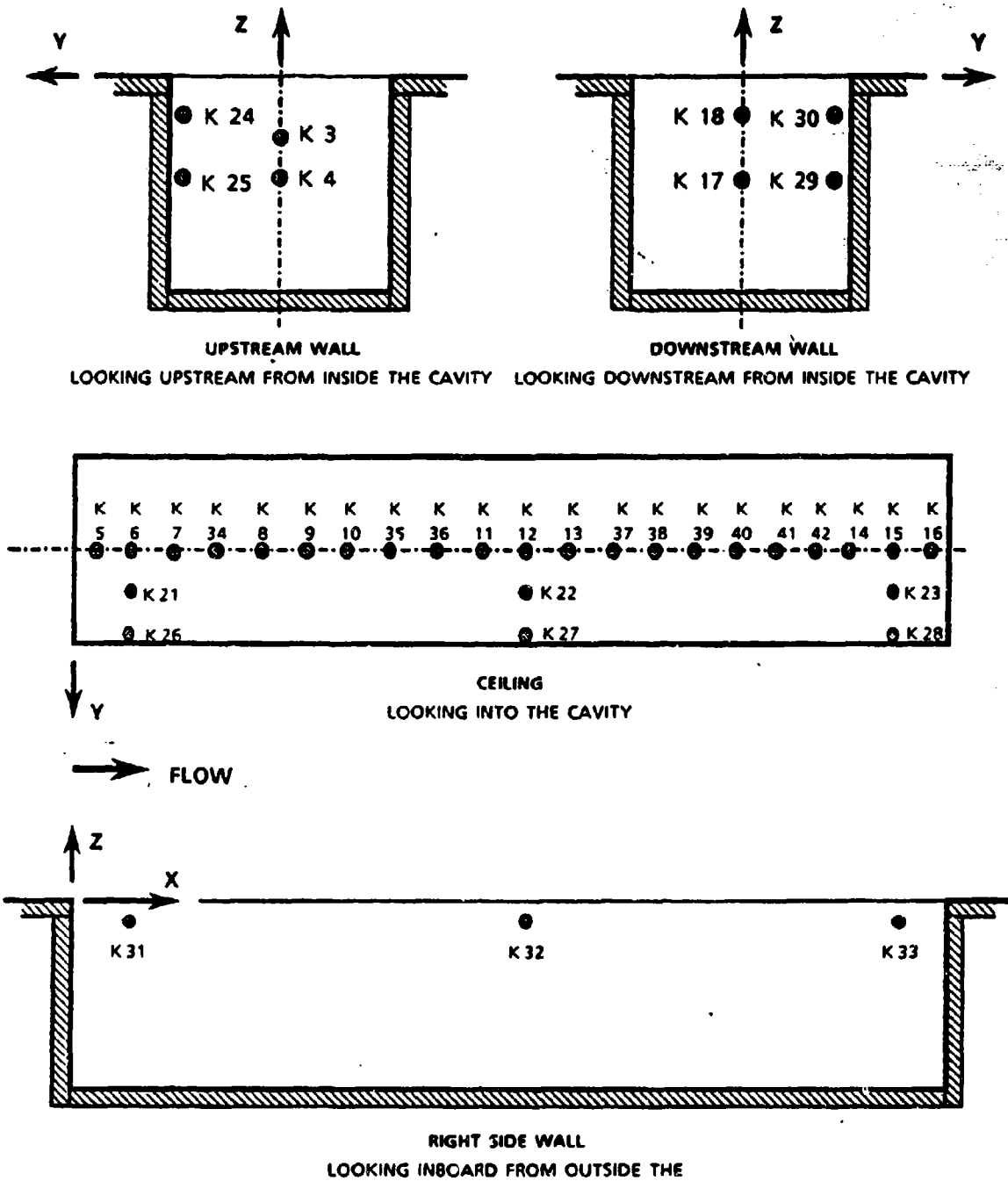

b. Location of pressure transducers in the cavity
Figure 24. Continued.

TRANSDUCER NUMBER	X MODEL INCHES	X/L	Y MODEL INCHES	Y/W/2	Z MODEL INCHES	TRANSDUCER NUMBER	X MODEL INCHES	X/L	Y MODEL INCHES	Y/W/2	Z MODEL INCHES
K 1	−3.175	−0.176	0	0	0	K26	1.075	0.060	1.8	0.90	−H
K 2	−0.475	−0.026	0	0	0	K27	9.175	0.510	1.8	0.90	−H
K 3	0	0	0	0	−1.125	K28	16.925	0.940	1.8	0.90	−H
K 4	0	0	0	0	−1.975	K29	18.000	1.000	1.9	0.95	−1.975
K 5	0.275	0.015	0	0	−H	K30	18.000	1.000	1.9	0.95	−0.725
K 6	1.075	0.060	0	0	−H	K31	1.075	0.060	2.0	1.00	−0.35
K 7	1.975	0.110	0	0	−H	K32	9.175	0.510	2.0	1.00	−0.35
K 8	3.775	0.210	0	0	−H	K33	16.925	0.940	2.0	1.00	−0.35
K 9	4.675	0.260	0	0	−H	K34	2.875	0.160	0	0	−H
K10	5.575	0.310	0	0	−H	K35	6.475	0.360	0	0	−H
K11	8.275	0.460	0	0	−H	K36	7.375	0.410	0	0	−H
K12	9.175	0.510	0	0	−H	K37	10.975	0.610	0	0	−H
K13	10.075	0.560	0	0	−H	K38	11.875	0.660	0	0	−H
K14	16.025	0.890	0	0	−H	K39	12.775	0.710	0	0	−H
K15	16.925	0.940	0	0	−H	K40	13.675	0.760	0	0	−H
K16	17.725	0.985	0	0	−H	K41	14.575	0.810	0	0	−H
K17	18.000	1.000	0	0	−1.975	K42	15.475	0.860	0	0	−H
K18	18.000	1.000	0	0	−0.725	K43	21.950	1.219	0	0	0
K19	18.875	1.049	0	0	0	K44	23.950	1.331	0	0	0
K20	20.275	1.126	0	0	0	K45	25.950	1.442	0	0	0
K21	1.075	0.060	0.9	0.45	−H						
K22	9.175	0.510	0.9	0.45	−H	K46	TUNNEL WALL				
K23	16.925	0.940	0.9	0.45	−H						
K24	0	0	1.9	0.95	−0.725	K101	GMPM STORE MODEL (See Fig. 11)				
K25	0	0	1.9	0.95	−1.975	106					

c. Pressure transducer locations

Fig. 24. Concluded.

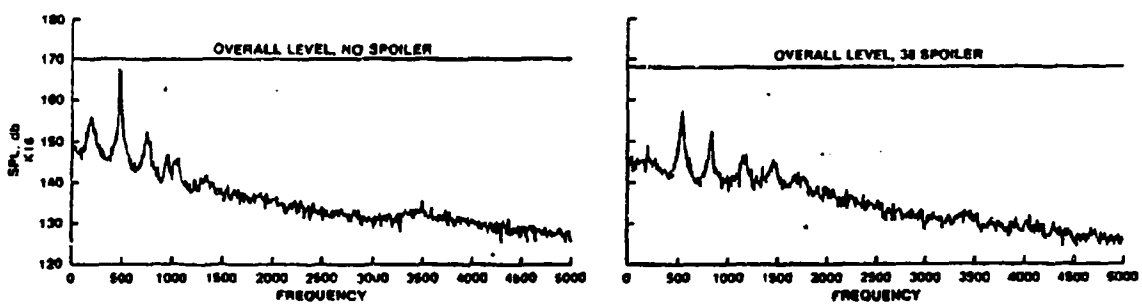

a. Fine sawtooth spoiler

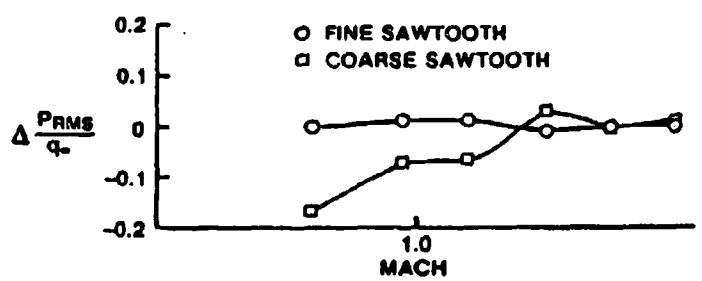

b. Comparison of fine and coarse sawtooth spoilers

Fig. 25. Effectiveness of 38 sawtooth spoilers, deep cavity (L/H = 4.5), transonic condition.

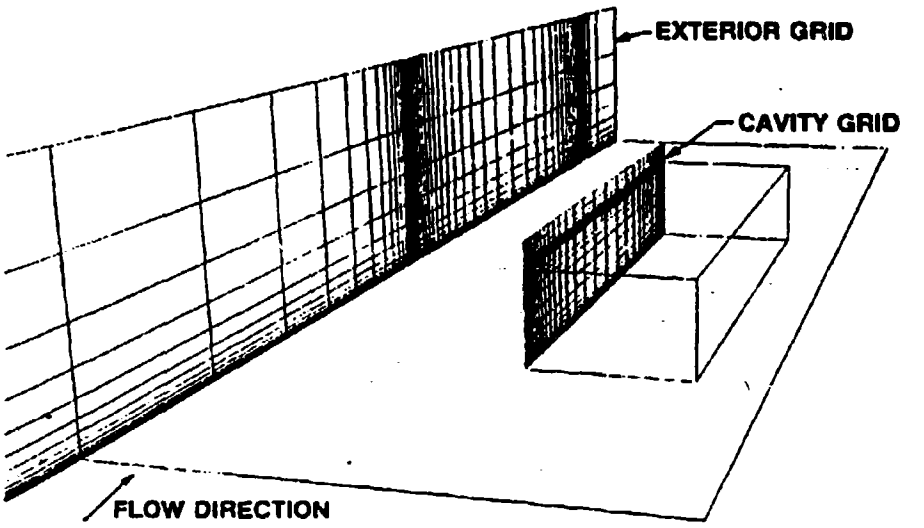

Fig. 26. Computational grids for a generic cavity (Ref. 9).

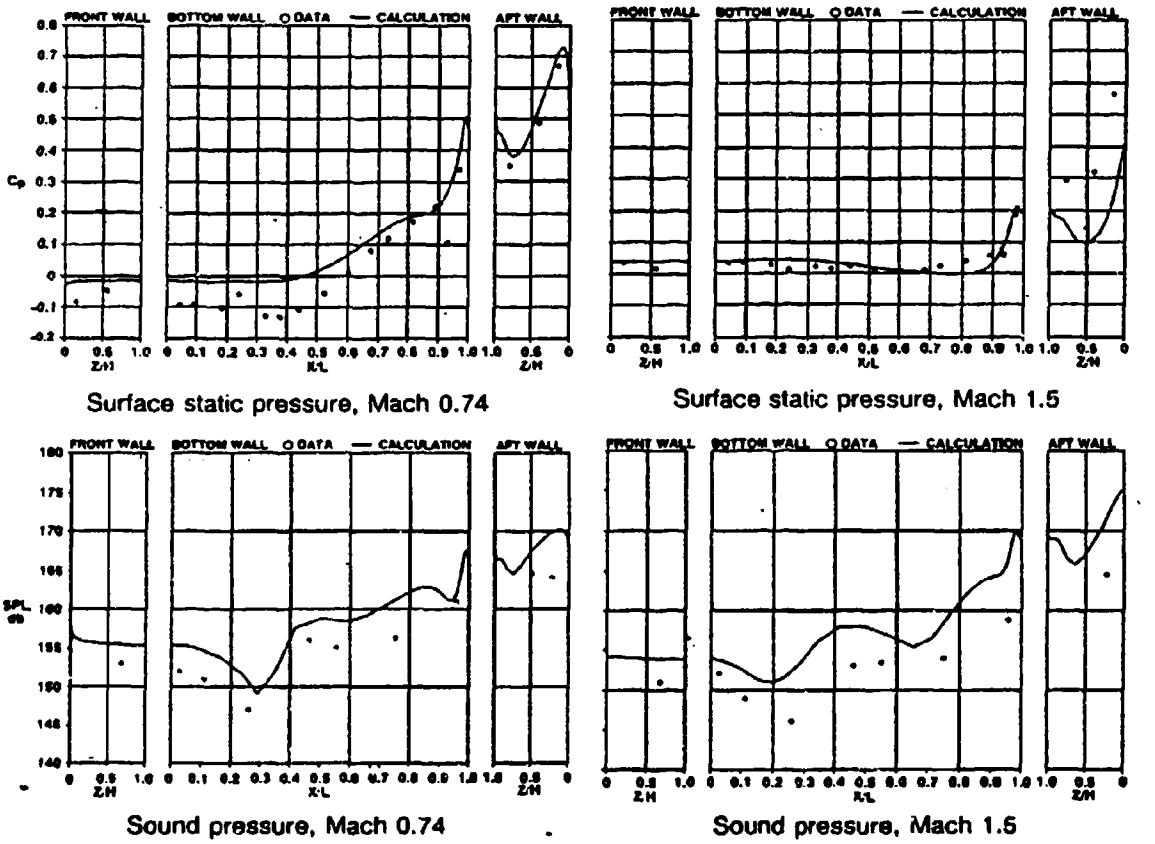

Surface static pressure, Mach 0.74

Surface static pressure, Mach 1.5

Sound pressure, Mach 0.74

Sound pressure, Mach 1.5

Fig. 27. Comparison of calculated and measured static pressure and sound pressure levels for a deep cavity (L/H = 5.6) (Ref. 9).

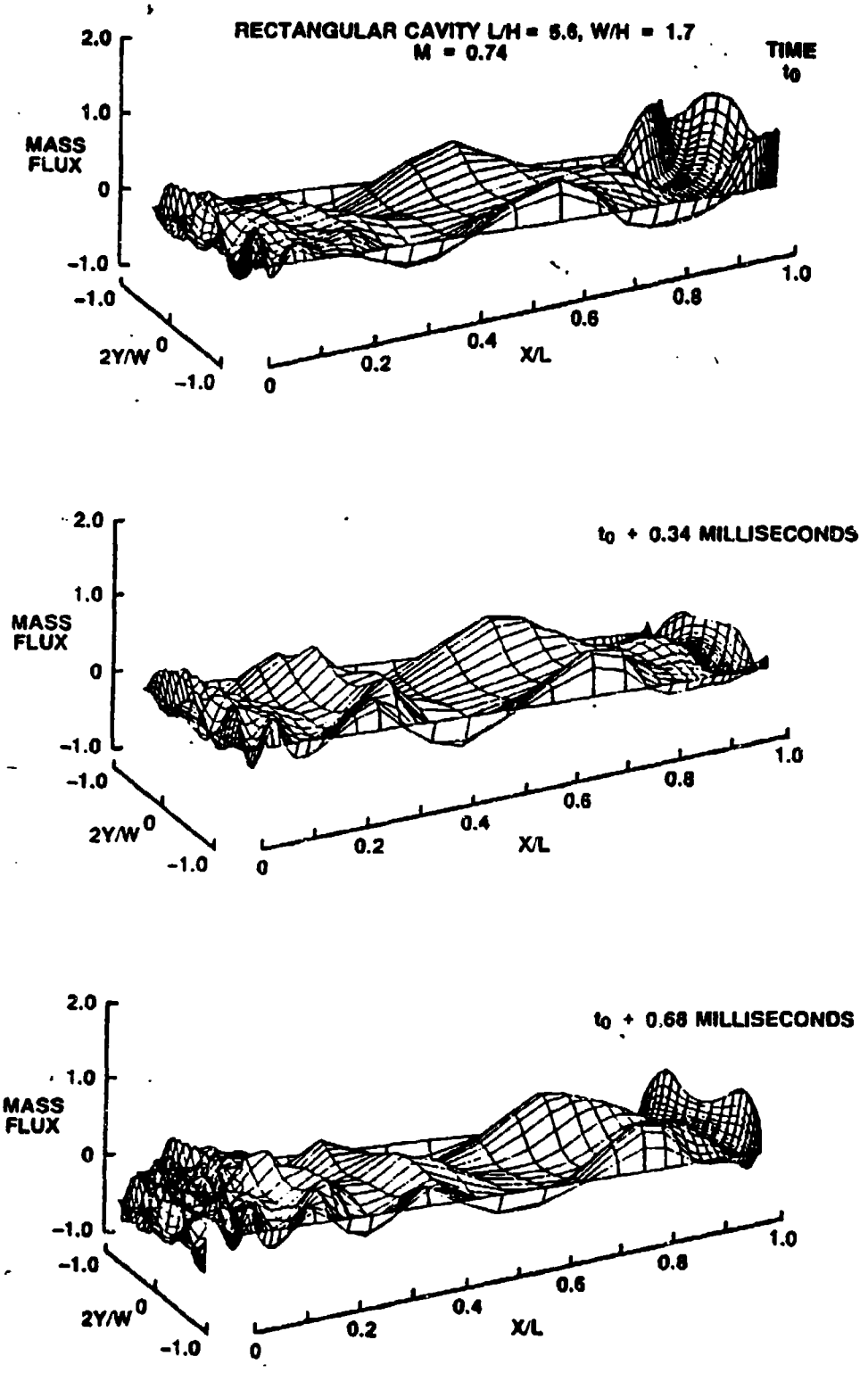

Fig. 28. Predictions of mass flux in the plane of a rectangular cavity opening (L/H = 5.6) at M = 0.74 (Ref. 9).

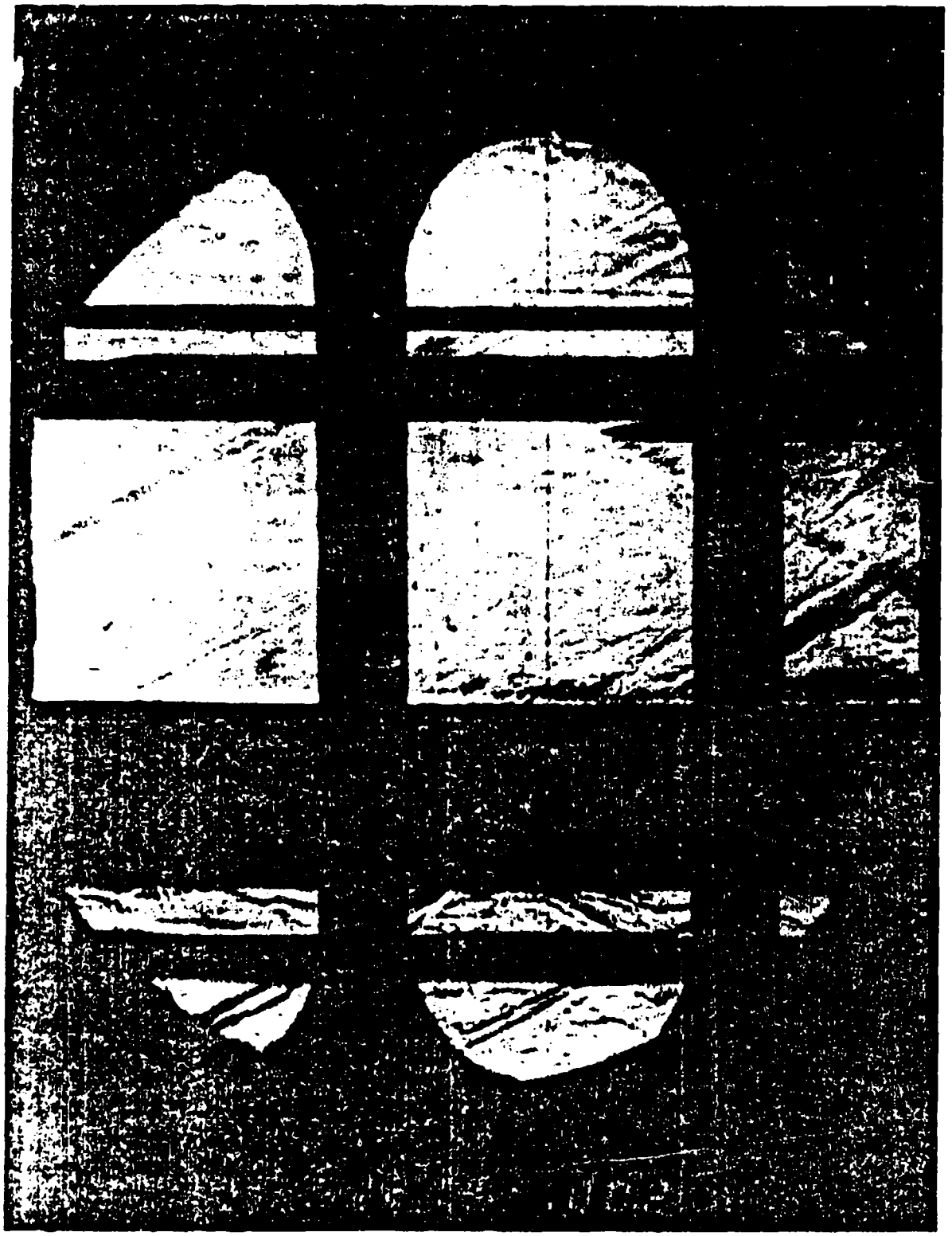

a. Clean cavity

Fig. 29. Schlieren photographs of flow over a transitional cavity (L/H = 9.0) equipped with various spoiler and door configurations.

b. Cavity with 3δ sawtooth spoiler at leading edge of cavity
Fig. 29. Continued.

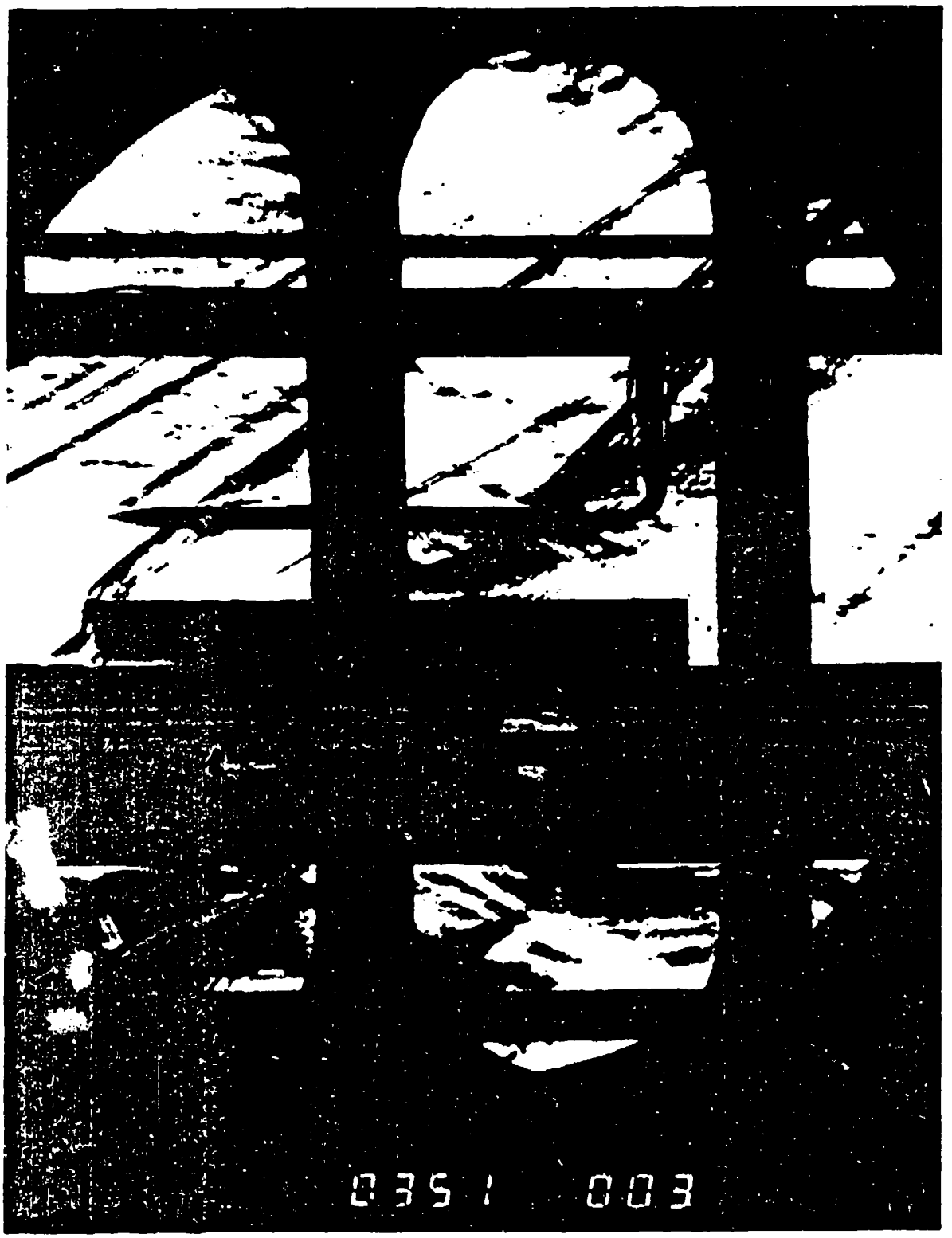

c. Cavity with SC 90 doors and 3δ sawtooth spoiler
Fig. 29. Continued.

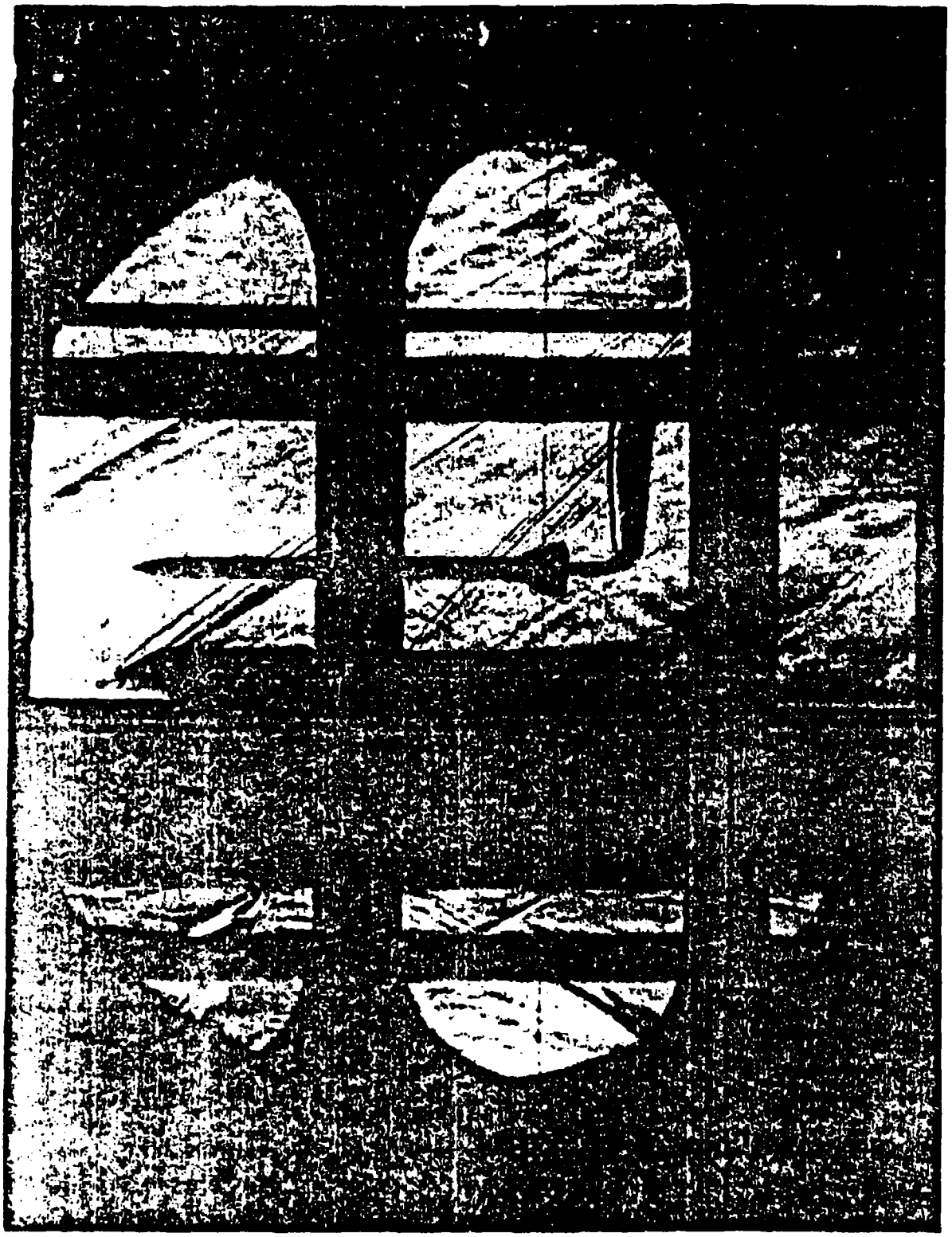

d. Cavity with TC 120 doors and 1δ sawtooth spoiler
Fig. 29. Concluded.

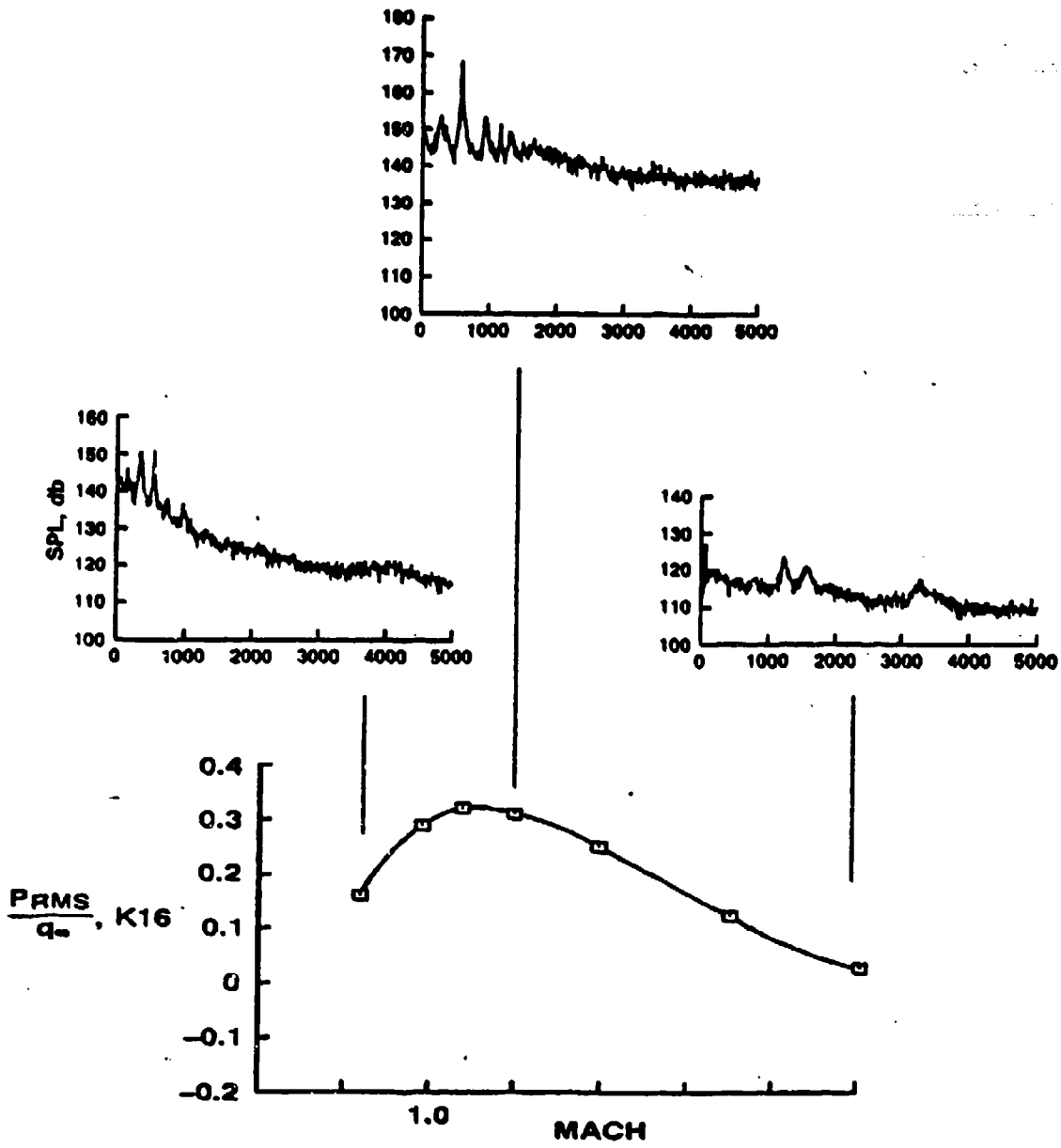

Fig. 30. Variation with Mach number of tonal amplitiudes and overall sound pressure levels in a deep cavity (L/H = 4.5) with no spoilers or doors.